



UPPSALA  
UNIVERSITET

UPTEC W 24047

Examensarbete 30 hp

Oktober 2024

# Application and use of CoastSnap data for shoreline modelling and research on coastal erosion

---

Therese Larsson & Frida Junegard



UPPSALA  
UNIVERSITET

## Application and use of CoastSnap data for shoreline modelling and research on coastal erosion

---

Therese Larsson & Frida Junegard

### **Abstract**

Coastal erosion is an increasing threat to shorelines and sandy beaches worldwide, while at the same time, field studies and monitoring can be both time consuming and expensive. In this report, community-collected data is used to conduct research on the shorelines on Australia's East Coast.

The community-collected data utilized for this research is smartphone images collected by the public to the citizen-science project CoastSnap. The report is divided into two parts, with the combined aim to gain more knowledge on erosion on Australia's East Coast, as well as understanding how well CoastSnap data can be used for this kind of research.

CoastSnap data was also tested and analyzed with the ShoreFor model which is a hindcasting model used to evaluate if data from CoastSnap can be used to predict future shoreline change. The first part aims to look at the beach erosion following the last La Nina event. This, due to La Nina's typical enhancement of precipitation and cyclones over Australia leading to coastal erosion.

The first part also aims, with the help of the hypothesis that the last La Nina event should erode the beaches on Australia's East Coast, with the results from the CoastSnap data, to see if the results are in line with previous research in the field. This together with analysis of the quantity of data worked as a base for answering the question "Can citizen data from Coastsnap show the effects on the shorelines of Australia's East coast from the Last La Niña period?". The second part aims to assess whether shoreline data collected from one CoastSnap site can drive the shoreline model ShoreFor, as this has never before been done with community collected data before.

The results proves that citizen data from CoastSnap provided reliable results regarding beach erosion on Australia's East coast during the last La Niña period, as it showed that erosion has been increasing in line with what has been proved in previous observations. It also shows that CoastSnap data can drive the ShoreFor model and that the hindcast results are concluded reliable. When testing the model performance by degrading the shoreline data, the model was quite sensitive to data sampling duration but not as sensitive to sampling frequency

**Teknisk-naturvetenskapliga fakulteten**

**Uppsala universitet, Utgivningsort Uppsala/Visby**

Handledare: Dr. Kristen D Splinter & Dr. Mitchell Dean Harley Ämnesgranskare: Thomas Stevens

Examinator: Fritjof Fagerlund

# Preface

We would like to send thanks to our wonderful supervisors, Dr. Mitchell Harley and Dr. Kristen Splinter, for giving us the opportunity to undertake this project and for making us feel at home away from home. A special thanks also goes to UNSW and the Water Research Laboratory in Sydney for welcoming us with open arms.

We would like to thank our subject reviewer from the Department of Geosciences in Sweden, Thomas Stevens. We also extend our heartfelt gratitude to Uppsala University for allowing us to undertake this project and for providing us with this incredible experience. And a big thank you to "Sveriges Ingenjörer" for awarding us a scholarship for environmental research, which helped fund this project.

Lastly, we want to thank our families for their unwavering support throughout the years and for always encouraging us to dream big. We also want to thank all the wonderful friends we made along the way; you have made all the hard work worthwhile. Thank you for making our years at Uppsala University so memorable. None of this would have been possible without you.

## Author Contributions

The sections on background and general methodology (Chapters 1–5.1.2) were developed jointly by both authors. Part 1 of the methodology, results, and discussion sections was authored by Frida Junegard, while Part 2 of the methodology, results, and discussion sections was authored by Therese Larsson.

Copyright © Therese Larsson & Frida Junegard, Department of Earth Sciences, Uppsala University.  
UPTEC W 24047, ISSN 1401-5765  
Digitally published in DiVA, 2024, via the Department of Earth Sciences, Uppsala University.  
(<http://www.diva-portal.org/>)

# Referat

## Tillämpning och användning av CoastSnap-data för strandlinjemodellering och forskning om kusterosion

*Therese Larsson och Frida Junegård*

Här följer en svensk sammanfattning av vad som är refererat till "Abstract" ovan.

Kusterosion är ett växande hot mot kuster och sandstränder världen över, men samtidigt kan fältstudier och övervakning för att tackla problemen vara både tidskrävande och kostsamma. I denna rapport används data insamlad av allmänheten för att bedriva forskning om kusternas förändring på Australiens östkust. Den samhällsinsamlade datan som används för denna forskning är bilder tagna med smartphones som samlats in av allmänheten till medborgarprojektet CoastSnap.

Rapporten är uppdelad i två delar, med det gemensamma syftet att öka kunskapen om erosion på Australiens östkust, samt att förstå hur väl CoastSnap-data kan användas som data i denna typ av forskning. CoastSnap-datan analyserades även med hjälp av ShoreFor-modellen, som är en hindcasting-modell som används för att utvärdera om data från CoastSnap kan användas för att förutsäga framtida förändringar av kuster.

Den första delen syftar till att undersöka stranderosionen efter den senaste La Niña-perioden. Detta på grund av La Niñas karakteristiska ökning av nederbörd och cykloner över Australien, vilket tenderar att leda till ökad kusterosion. Den första delen syftar också på, med hjälp av hypotesen att den senaste La Niña-händelsen borde ha eroderat stränderna på Australiens östkust, att med resultaten från CoastSnap-data se om dessa överensstämmer med tidigare forskning på området. Detta tillsammans med en analys av datamängden fungerade som grund för att besvara frågan "Kan medborgardata från CoastSnap visa effekterna på kusterna på Australiens östkust från den senaste La Niña-perioden?".

Den andra delen syftar till att bedöma huruvida kustdata insamlad från en CoastSnap-station kan driva kustmodellen ShoreFor, vilket aldrig tidigare har gjorts med data insamlad från allmänheten.

Resultaten visar att medborgardata från CoastSnap gav tillförlitliga resultat angående kusterosion på Australiens östkust under den senaste La Niña-perioden, då det visade att erosionen har ökat i linje med vad som bekräftats i tidigare observationer. Det visar också att CoastSnap-data kan driva ShoreFor-modellen och att hindcast-resultaten bedöms vara tillförlitliga. När modellens prestanda testades genom att försäkra kystdata, visade sig modellen vara ganska känslig för datainsamlingsperiodens längd men inte lika känslig för insamlingsfrekvensen.

*Institutionen för geovetenskaper, Uppsala. Villavägen 16, 752 36 Uppsala, Sweden*

# Populärvetenskaplig sammanfattning

Australiens kustlinje med dess sandstränder är uppskattade av såväl lokalbefolkning som turister. Tyvärr är stränderna under hot av omfattande erosion till följd av bland annat klimatförändringarna. För att på bästa sätt kunna skydda dessa områden är det av största vikt att förstå hur kusten och strandlinjerna förändras samt ta reda på de drivande faktorerna. Detta för att på bästa sätt kunna förutse framtida förändring och på så sätt kunna agera förebyggande.

Syftet med denna studie är att undersöka strandlinjeförändringar längs Australiens östkust. Detta för att dra slutsatser kring hur klimatfenomenet ENSO har påverkat stränderna samt förutsäga framtida förändringar av kustlinjen. Detta görs i denna studie med data insamlat från allmänheten i form av fotografier. Studiens resultat visade att under den senaste La Niña-fasen, en fas i klimatvariationen ENSO, drog sig strandlinjerna på Australiens östkust tillbaka. Studien visar också att bilder insamlade av allmänheten kan användas som data vid analys av tidigare erosion samt för att förutse framtida erosion med hjälp av ett modelleringsverktyg som kallas ShoreFor. Detta framstår som ett bra alternativ till mer kostsamma och tidskrävande metoder.

Stranderosion är den process där stränder förlorar massa och strandlinjer flyttar sig närmare land. Detta kan skapa stora problem för många samhällen, inklusive stora hot mot infrastrukturen nära stränderna. Forskning inom området är viktigt för att beslut om åtgärder samt förebyggande insatser ska kunna tas på grundade beslut. Studien understryker de växande miljöhoten från kusterosion, inklusive förlust av mark och egendom, habitatförändringar och förstörelse av infrastruktur. Klimatförändringar, såsom stigande havsnivåer och ökade stormar, förväntas förvärra kusterosionen. Ett exempel är La Niña-perioder som 2010/2011 orsakade förödande regn och översvämningar i Australien. ENSO är en klimatvariation som uppstår över Stilla havet. ENSO växlar mellan 'normala' förhållanden, La Niña och El Niño. Dessa faser är kopplade till de passadvindarna som finns över Stilla havet och deras inverkan på det varma havsytvattnet. Vattentemperaturen påverkar i sin tur temperatur, nederbörd och intensiteten av stormar på kontinenterna på var sida om Stilla havet. Beroende på vilken ENSO-fas som råder, kan olika effekter förstärkas. Under La Niña förväntas mer nederbörd och kraftigare stormar som cykloner över Australien, vilket bidrar till ökad stranderosion. I och med detta är ENSO-perioderna intressanta att undersöka.

Att samla in data till denna typ av forskning har länge varit en dyr och tidskrävande process. Ett alternativ som undersökts i denna studie är data som samlats in av allmänheten genom CoastSnap. Detta är intressant för forskare och myndigheter att utforska för att se om medborgarsamlade data kan användas i studier av stranderosion. Om så är fallet kan mer data samlas in med mindre resurser. Detta skulle innebära att en större omfattning av värdefull forskning skulle kunna genomföras, vilket skulle hjälpa till att förutse framtida scenarion och därigenom möjliggöra bättre beslut för att skydda strandlinjerna och närliggande samhällen.

Tidigare forskning tyder på att stränder som är särskilt utsatta för erosion gynnas av att ha data som samlas in månadsvis. Medborgarsamlat data kan vara fördelaktigt här eftersom det inte krävs ytterligare engagemang eller finansiella medel för att samla in mer data. Den huvudsakliga nackdelen som identifierats i denna rapport och i andra studier om medborgarsamlat data är att frekvensen och exaktheten i tidpunkten för datainsamling inte lätt kan styras eller kontrolleras. Medborgarsamlat data genom CoastSnap är också ett effektivt sätt att utbilda och engagera allmänheten i frågor och risker som är förknippade med kusterosion.

Forskningen i rapporten utfördes i två delar, där båda delarna använder fotografier inskickade av allmänheten till CoastSnap. Med hjälp av förutbestämda referens-GPS-punkter kunde bredden på strandlinjen mätas. Strandlinjen markerades sedan i varje bild för att få en datauppsättning för varje bilds strandlinjebredd.

Den första delen av studien analyserades data från sju stränder under perioden som definierar den senaste La Niña-händelsen. Resultaten jämfördes med tidigare forskning för att se om de stämde överens med förväntningarna baserat på tidigare studier och teorier. Datakvaliteten och mängden data analyserades också tillsammans med resultaten för att avgöra tillförlitlighet hos insamlade datan och resultatet. I den andra delen testades den insamlade kustlinjedatan från CoastSnap i ett modelleringsverktyg vid namn ShoreFor. Detta verktyg förutsäger hur kustlinjen kan tänkas att förändras i framtiden genom att analysera tidigare förändringar av strandlinjen. Även om kustmodellering inte är nytt, är användningen av offentliga data en innovativ metod. Data som användes i modellen inkluderade all tillgänglig CoastSnap-data från en strand, och vågdata hämtades från en databas kopplad till en boj längre ut till havs nära samma strand. Vågdatan modifierades genom programmering för att bättre passa parametrar närmare strandlinjen. Det omvandlade vågdatan från den närmare positionen var att föredra eftersom det matchade platsen där strandlinjedata insamlades. Eftersom programmet för omvandling inte var tillgängligt för alla användes båda typerna av vågdata för att utvärdera om omvandlingen var nödvändig.

# Contents

1	Introduction . . . . .	1
2	Problem and purpose . . . . .	1
2.1	Problem description and purpose . . . . .	1
2.2	Research questions . . . . .	3
2.2.1	Part 1: Impacts of La Niña . . . . .	3
2.2.2	Part 2: Shoreline modeling . . . . .	3
3	Background . . . . .	3
3.1	Characteristics and coastal processes of the Australian East Coast . . . . .	3
3.1.1	Coastal types of the Australian East Coast . . . . .	4
3.1.2	Sand transport . . . . .	6
3.1.3	Erosion and deposition . . . . .	7
3.1.4	Managment of coastal erosion . . . . .	8
3.2	What drives the sand transport? . . . . .	9
3.3	Waves, and their driving forces . . . . .	10
3.4	La Niña, Cyclones, and the effects on beach erosion . . . . .	11
3.5	Coast Snap and citizen collected data . . . . .	14
3.5.1	Data . . . . .	17
3.6	Shoreline modeling . . . . .	17
3.6.1	Empirical equilibrium cross-shore models . . . . .	18
3.6.2	The ShoreFor model . . . . .	19
4	Study sites . . . . .	19
4.1	Alexandra Headland beach . . . . .	20
4.2	Buddina Beach . . . . .	21
4.3	Stockton Beach . . . . .	23
4.4	Blacksmiths Beach . . . . .	25
4.5	North Narrabeen Beach . . . . .	27
4.6	Manly beach . . . . .	29
4.7	Broulee Beach . . . . .	33
5	Methodology . . . . .	35
5.1	General . . . . .	35
5.1.1	Collecting of Images . . . . .	36
5.1.2	Shoreline change and mapping . . . . .	36
5.2	Part 1: Impacts of La Niña . . . . .	39
5.2.1	Time frame . . . . .	40
5.2.2	Choosing a site . . . . .	40
5.2.3	Data selection . . . . .	40
5.2.4	Timeseries . . . . .	41
5.3	Part 2: Shoreline modeling . . . . .	42
5.3.1	Data generation . . . . .	42
5.3.2	ShoreFor GUI v1.0 setup . . . . .	44
5.3.3	Model Inputs . . . . .	45
5.3.4	Initial model . . . . .	45
5.3.5	Test cases . . . . .	45
5.3.6	Test result analysis . . . . .	47

6	Results . . . . .	49
6.1	Part 1: Impacts of La Niña . . . . .	49
6.1.1	Alexandraandra Headland Beach . . . . .	49
6.1.2	Buddina Beach . . . . .	51
6.1.3	Stockton Beach . . . . .	52
6.1.4	Blacksmiths Beach . . . . .	54
6.1.5	North Narrabeen Beach . . . . .	56
6.1.6	Manly Beach . . . . .	58
6.1.7	Broulee Beach . . . . .	60
6.1.8	Combined results . . . . .	61
6.1.9	Data distribution . . . . .	62
6.2	Part 2: Shoreline modeling . . . . .	63
6.2.1	Initial model . . . . .	63
6.2.2	Test cases . . . . .	64
7	Discussion . . . . .	69
7.1	Part 1: Impacts of La Niña . . . . .	69
7.1.1	Time-series . . . . .	69
7.1.2	Data distribution . . . . .	72
7.1.3	Error analysis . . . . .	73
7.1.4	For future studies . . . . .	73
7.1.5	Conclusions . . . . .	74
7.2	Part 2: Shoreline modeling . . . . .	74
7.2.1	Initial model . . . . .	74
7.2.2	Test cases . . . . .	74
7.2.3	For future studies . . . . .	76
7.2.4	Conclusions . . . . .	76
8	Bibliography . . . . .	77

# 1 Introduction

Australia's sandy beaches are renowned worldwide and highly valued by both locals and tourists. However, these beaches and coastal communities face a significant threat from coastal erosion. Beach erosion and shoreline recession are natural processes that affect shorelines around the globe to varying degrees, although the events of human activities, particularly those related to climate change, can increase the magnitude of the situation.

The infrastructure is significantly threatened by beach erosion in locations of the world which experiences it more severally (Finkl, 2013). According to the National Oceanic and Atmospheric Administration extreme weather events and coastal disasters for instance in 2012 alone, resulted in over \$110 billion in damages in the U.S., with Hurricane Sandy accounting for approximately \$65 billion of that amount. (NOAA 2015)It is predicted that erosion may destroy 1/4 of the houses within 150 m of the shoreline over the coming 60 years (Finkl, 2013). These examples relate to the United States but equal threats are facing the Australian coastline. Williams (2017) highlights the possible financial losses following consequences which hits tourism, which is a great and important asset to the Australian economy. To improve the chances of protecting the future coastal communities and shorelines research is important in the area.

This study aims to investigate new ways to contribute to this area of study in order to proactively prepare coastal areas in risk of erosion. The data used for this purpose is provided from the relatively new community-based project called CoastSnap. The data will be used both for analyzing past events, as well as testing the data in the hindcasting shoreline model ShoreFor, which has never before been done with community-collected data.

## 2 Problem and purpose

In this section the purpose of this report as well as the problem description will be presented. The report will be divided into two main parts, introduced in the section below. These parts will have separate research questions and approaches which in combination will serve the purpose of this report.

### 2.1 Problem description and purpose

Beach erosion affects coastlines all over the world and with growing populations and desire to exploit the coastlines, management and research on the worlds coastlines becomes all the more important (Williams, 2017). Australia is known for its iconic sandy beaches and coastal areas all over the world, which contributes greatly to the GDP, mainly through the high stream of tourism (Williams, 2017). The biggest threat to coastal communities due to beach erosion is the loss of land and property, threatening both the economy and safety for both locals and tourists (Hanson, 1993). The coastal areas are also an important part of the ecosystem as it provides important services and processes many ecological values (James, 2000). For example, coastal erosion can release stored carbon in soils present in the coastal ecosystems, becoming a feedback mechanism to global warming (Spivak, 2019)

Both direct human-induced processes, such as exploitation, mining, and coastal development, as well as indirect effects, like sea-level rise due to global warming, pose threats to coastal environments (Defeo, et al., 2008). With climate change, natural processes such as storms are expected to increase in both frequency and severity, consequently heightening the risk of coastal erosion (Walsh, et al., 2015). One of these climate oscillations, called ENSO, hovers over the pacific ocean mainly affecting the southern coastline of South America and northern coastline of Australia and causes more storms, extreme rainfall and cyclones in some periods (Komarl, et al., 2000). These periods are called La Niña. During one of the latest registered La Niña periods, occurring between 2010 - 2011, Australia experienced storms so severe that the consequences were devastating. The following floods of the extreme rainfall claimed 35 lives, and left damage worth billions of dollars (Ummenhofer, et al., 2015) .

Research on coastal erosion can be done in many different ways. A lot of surveys done to monitor coastal change can be expensive and impractical to conduct at the frequency desired (Smith and Benson, 2001). An alternative to expensive and time consuming beach surveys is citizen collected data, which in the case of a project called CoastSnap implies photographs collected by the community. The citizen-science project CoastSnap was founded between NSW Department of planning, Industry and Environment and UNSW Water Research Laboratory as a pilot project in 2017, operating by collecting data from the community (CoastSnap, 2023a). Citizen collected data has a lot of benefits. In the case of CoastSnap, the data is collected with citizens smartphones, therefore the only cost being the instruction-sign and stainless steel cradle (for positioning the smart phone) that is implemented at a specific site overlooking the beach. The managing of the site is minimal and not time consuming at all, and as the public collects the images no expensive equipment is needed. Another great benefit of using CoastSnap is the involvement of the community by raising awareness for educational purposes.

Naturally, collecting data from the community also comes with challenges. Performing reliable data analyses often require a certain amount of desired data, which is something that can't be controlled in the same way as if the researcher/s in question is responsible for the data collection, as it in this case is dependent on citizens submitting the data on their free time with their private smartphones. Therefore the sampling frequency is the result of several unpredictable conditions, such as weather or season, that affects number of visitors at the CoastSnap sites as well as the personal will to participate.

To study beach erosion, in this project, data from CoastSnap will be used both for modeling the future shoreline changes and for analysing past conditions during the latest La Niña event.

The aim of this study is to examine to what extent citizen collected data can be used for analysing past shoreline conditions as well as modeling changes in the future. For the analysing part, data from the lates La Niña event will be used. This will be accomplished by testing if the CoastSnap data corroborates with the assumed hypothesis formed from previous studies and knowledge that La Niña should increase erosion. CoastSnap data from one of the study sites will also be used to model the possible future with the modeling program Shorefor, which is a hindcasting model, to examine whether CoastSnap data can be used to predict future shoreline change.

## **2.2 Research questions**

This study is divided into two main parts - Part 1: "Impacts of La Niña" and Part 2: "Shoreline modeling". The specific research questions for both parts are presented below.

### **2.2.1 Part 1: Impacts of La Niña**

"Can citizen data from CoastSnap show reliable results regarding beach erosion on Australia's East coast during the Last La Niña period?"

In this part, an investigation was conducted to assess the effectiveness of CoastSnap data in analysing past beach erosion events. The focus was to utilize the CoastSnap data to examine the impact of the last La Niña event on the shorelines of Australia's east coast. Following research questions was addressed:

1. Are the results showing what is expected from the theory about ENSO and coastal erosion?
2. From the results, and from previous research, is the data sufficient to draw conclusions about the degrees of coastal erosion in the researched area?

### **2.2.2 Part 2: Shoreline modeling**

"Can citizen data from CoastSnap be used to model the future shoreline conditions?"

The primary focus of the second part of this thesis is to assess the extent to which citizen science data can drive the ShoreFor model for forecasting future shoreline changes. This inquiry will be divided into 2 key questions:

1. How much data from CoastSnap is needed to train ShoreFor v1.0?
2. Is inshore/local wave conditions needed in order to get good model results when training the ShoreFor model with CoastSnap data?

## **3 Background**

The main focus of this report was the effects of shoreline change, and more specifically shoreline retreat. Background information on the processes that cause and drive shoreline recession is presented in this section. Theory mainly on Australia's coastal types, sand transport and beach erosion, as well as background information on CoastSnap and the ShoreFor model is included.

### **3.1 Characteristics and coastal processes of the Australian East Coast**

In this section the characteristics and the coastal processes of the Australian east coast is introduced. This includes the southern half of the east coast since this is the region where the 7 study sites are located.

### 3.1.1 Coastal types of the Australian East Coast

The 7 sites in this report are located in two different geographical regions, referred to as Central East region and Southern New South Wales (NSW) region (Short, 2020). The study site furthest to the north is Alexandra Headland beach which is located on an longitude of 153.10804, about 100 km north of Brisbane. Alexandra and Buddina are located in the Central East Region, while the other 5 remaining beaches in this report resides in the Southern NSW region (Short, 2020). The Central East region reaches from the northern part of the NSW Coast to the south of Queensland while The Southern NSW region extends along the coast for about 1000 km between Cape Howe and Cape Hawake. Both regions have a mix of sandy and rocky beaches and several headlands are present, dividing the beaches and shorelines from each other. In figure 1 the locations of the study sites are illustrated.



Figure 1: Illustration of the study site locations. Map base from freeworldmaps.net

All study sites are considered wave-dominated beaches and experiencing micro-tides (Short, 2020). The swell comes from the south, giving the highest waves with the most energy in the south part of the coast and less so the further north traveled (Short 2020).

Both of these regions experience a highly variable wave-wind climate but an high-energy swell is

always present and the beaches in both regions are classified as high energy beaches (Short, 2020). According to a study by Wright, et al. (1979), when this is the case two different kinds of beach systems generally occur: (1) reflective systems; and (2) dissipative systems. The study was made with field experiments where measurements of the currents, circulation patterns and depositional morphology were replicated for several locations in the New South Wales region for different energy conditions. The result in the study is a general model for the variations of the systems present in this region. One thing to emphasise is the great variation in dynamics and the wide range of morphology in the NSW region. Big contrasts in beach behaviour are seen between even neighbouring beach compartments. Because of this a large part of the research and literature present on morphologies and hydrodynamic relationships from different parts of the world are applicable on the coastal areas of New South Wales.

The seven study sites used in this study are located in regions where the beaches are wave dominated and both reflective systems and dissipative systems are present. The dissipative system (D) is the system that develops on the higher end of the energy spectrum when the waves are at their peak height, averaging around 2.5 m. While the reflective beaches (R) refer to the systems that occur on the lower energy part of the spectrum when the waves drop below 1 m. In between these energy levels, different kinds of intermediate systems develop. These are referred to as Longshore Bar and Trough (LBT), The Rhythmic Bar and Beach (RBB), Transverse Bar and Rip (TBR) and the Low Tide Terrace (LTT). In the context of coastal geography, a **bar** refers to a submerged or partially submerged ridge of sand or other sediments that is usually parallel to the shoreline. It often forms offshore and influences the behavior of waves and currents. **Trough** refers in this case to a long, narrow depression or channel. This area is often located between sandbars or offshore ridges and often contain circulating currents (Short 2020).

The dissipative system is exposed to the open coast and the profile of the system has a flat and wide surf zone. The swell is on average 2-3 meters and the waves break 75-300 m seaward. When the waves break in this kind of system, most of the wave energy is depleted before they reach the beach. This causes a significant gradient in the flux of momentum carried by the waves, called the radiation stress gradient. The topography for dissipative beaches are usually relatively complex and varied. It often contains one or several bars and rip cells of different scales and complex three-dimensional inshore topography is generally present. These systems generally have a strong bed return flow (Wright, et al., 1979).

Different from the dissipative systems the reflective systems have steep and linear beach faces. The beaches are also characterized by well-formed beach cusps (shoreline formations in an arc pattern) and berms. The system also encounters surging breaks, characterized by waves rolling onto the beach, along with strong run-up and backwash. Different from the dissipative beaches the reflective beaches does not experience rip cells and the associated three-dimensional inshore topography (Wright, et al., 1979).

As mentioned earlier, between these two states on either side of the energy spectrum there are intermediate systems. (LBT) develops when the waves are slightly lower, around 2-2.5 m, or when the sand is finer. The Longshore Bar and Trough, typically have an outer bar that's set apart from the beach by a broad and deep trough. This trough often contains a circulating **rip current**. Rips are what develops when water that has been transported by the waves gets carried back out at sea. They exist as narrow strong currents, often confined between shallow sandbars flowing in

deeper channels. The rips get stronger with increasing wave height, as there is more water to be returned seawards (Short, 2020).

(RBB) occurs when waves decrease to a height of between 1.5-2 m. When this happens the bar moves towards the shore creating rip current circulation and **wave refraction** in the surf zone. Wave refraction refers to the changing and bending of the waves as they approach the shore. This happens as the different parts of a wave are influenced by varying depths of water. With the presence of both rip currents and wave refraction a highly rhythmic shoreline is created (Short, 2020).

When waves are around 1.5 m and the sandbars connect to the shoreline the Transverse Bar and Rip is created (TBR). When this occurs there are shallow transverse bars present close to the deeper rip channels. This will lead to a distinct pattern in the circulation where different rip currents are separated (Short, 2020).

As the waves decrease to 1 meter, the bar keeps moving toward the shore, and the rip channels start to fill up to create Low Tide Terrace (LTT). This terrace may have a connected low tide bar, and there's a chance it could be intersected by small remaining rip channels (Short, 2020).

### 3.1.2 Sand transport

The beaches and their ever dynamic states and forms are of main interest in this report and therefore since this is a study on sandy beaches, sand transport is the main area to understand. There are a number of processes that play a part in the movement of sand, both onshore and offshore. In the previous section the different kinds of beach systems found in wave-dominated high energy beach areas were demonstrated, including movement of sand depending on the type of sand, the morphology of the beach and how the water moves (waves, rips, tides etc). However, the morphology changes depending on the water movement and the waves and rips in turn change depending on the morphology of the beach. Swells and waves are also dependent on much larger scale systems like weather, seasons, storms, climate oscillations etc (Short, 2020).

A term often referred to with sand transport and erosion is **sediment budget**. The sediment budget of a system is the sum of all the sources adding and removing sediment from it. When the sediment budget is positive, sediment is added to the system in a higher rate than its being removed. When the sediment budget is negative, the opposite is true. The budget will also naturally oscillate between periods of negative budget and positive budget as it goes through periods with varying wave conditions. This cycle is called **beach oscillation**. These budgets are not easy to calculate, but an approximation can be formed based on the nature of the beach system, the location and the shoreline's long term observed behavior (Short, 2020).

When the beach has experienced a long-term positive sediment budget, the response will be what is called beach **accretion**. Accretion is what is referred to as beach recovery. **Beach recession** on the other hand refers to the net retreat of a shoreline, which is the consequence of a long-term negative sediment supply, and is what is referred to as beach erosion (Short, 2020).

A beach can experience recession and accretion simultaneously. This can happen when one side of the beach experiences periodic recession while the other side of the beach experiences accretion.

This phenomenon is called **beach rotation**. This occurs as a response to change in wave direction (Short, 2020).

Sand moving along the coastline is called **longshore sand transport**, and sometimes also referred to as littoral drift. Longshore sand transport can happen when breaking waves lift the sand from the sand bed and longshore currents induced by waves transport the sand along the coast. This especially happens when breaking waves are hitting the shore askew. The waves meet the shoreline at an angle then the backwash transports it back but now perpendicular to the shoreline. When the waves hit the shoreline in a bit of an angle towards it creates a net transport of sand along the shoreline. For the east coast the net transport goes towards the north as it experiences mostly waves from the south east. Although, the sand transport can change direction if the direction of the waves changes. If so, the net longshore transport will be determined by the sum of the opposing transport rates (Short, 2020).

Longshore transport can be obstructed by barriers like headlands. This is called **headland bypassing**. With headland bypassing the sand gets on the other side of the barrier by being transported under the water. This is different from **headland overpassing** where the sand is transported over the barrier with the wind. Due to the waves, currents and what are called megaripples, which are large underwater ripples, the sand can be shifted around the headland. As the longshore erosion generally goes towards the north on the east coast, the sand circulates around the headland from the south side towards the north. The transported sand will gradually merge with the beach on the other side of the headland and then continue to move along the shoreline (Short, 2020).

In the report "Sediment transport on dissipative, intermediate and reflective beaches" Aagaard, Greenwood and Hughes (2013) investigates the behavior of sand transport in different beach states, including dissipative, intermediate, and reflective beaches. The research was mainly done with field experiments. The experiments involved measuring suspended sediment fluxes on various beaches. For dissipative beaches they found that the net transport is typically offshore and decreases as it moves seawards. They also state that the rates of transport are relatively small, leading to slow changes in the morphology. They study also showed that if the local relative wave height becomes very large, the net transport can reverse. Fully reflective beaches have a very small net transport that is close to negligible, and they also experience a slow morphological change and the cross-shore transport gradients are not very pronounced. The intermediate beaches on the other hand are characterized by large cross-shore and alongshore transport gradients. It was also stated that high morphological variability and dynamic beach states are observed and for RBB and TBR the morphology is three-dimensional. A key factor from their findings relevant for this report is that maximum sediment transport rates are higher for intermediate beaches compared to dissipative and reflective beaches.

### 3.1.3 Erosion and deposition

According to Anthony (2017), beach erosion is a natural phenomenon characterized by the gradual loss of sediment from a beach, leading to a negative sediment budget. This occurs when the beach is unable to effectively counterbalance the energy generated by waves, currents, and accumulated water. In consequence, the beach will experience a net sediment loss. This sediment loss will cause the beach to lower and retreat. Essentially, beach erosion can be understood as the outcome of an imbalance between the energy inputs and the resistance offered by the beach bed and sediment

susceptible to change due to the forces of the ocean. Due to their composition of loosely packed, non-cohesive sediments, beaches serve as protective barriers that absorb, reflect, and disperse the energy brought to the shore by waves. Anthony (2017) also points out that beach erosion can both occur over a brief period from hours to months if the erosion is caused by events like storms or tsunamis, but it can also be a more prolonged process, spanning over several years, which indicates a gradual depletion of the beach sediment budget over time. As stated in the previous section, beach erosion can in this case also be referred to as beach recession.

Short (2020) explains that episodes where the coastal erosion is significant are most of the time connected with extreme weather events like flooding, surge and coastal storms. Tsunamis are also an event that create significant events of coastal erosion. In the event of a tsunami the waves and currents can reach landmass that are normally far from reach from the ocean, but the waves and currents typically also have a greater intensity which in itself contributes to more erosion. Tsunami events can easily lead to undercutting of cliffs and the creation of steep slopes and this will later often result in mass wasting. Heavy rainfall can also contribute greatly to coastal erosion as it enhances the saturation of soils. The high saturation leads to the shear strength of the soil being reduced, which increases the change of landslides as the slope fails to hold (Short, 2020).

The study "Synchronised patterns of erosion and deposition observed at two beaches" by Bracs et al. (2016) analyzed erosion at Wamberal and Narrabeen beaches in NSW, Australia, to determine if regional beaches behave similarly. Findings showed synchronized erosion and deposition patterns at both sites, suggesting regional coherence to environmental forces. This supports the use of "regionally representative" sites for cost-effective coastal monitoring. Data was collected through detailed monthly surveys and historical photogrammetry.

### **3.1.4 Management of coastal erosion**

Williams, et al. (2017) lists some of the advantages and disadvantages of a few coastal defence structure available, with the purpose to combat coastal erosion and protect the coastal areas. The most common options for managing coastal erosion available is, (1) groynes, (2) seawalls, (3) revetments rock armour, (4) offshore structures, and (5) sand dunes. (1) Groynes is a rigid structure that is built perpendicularly from the shoreline which maintains the beach level and intercepts long-shore sand movement. The structure is fast and easy to build. However, controlling cross shore sand movement is not the most effective solution and is costly and needs high maintenance. (2) Seawalls are vertical concrete or stone walls that acts as a barrier from the water and erosion. The advantage of these walls are that they can resist severe exposure. The main cons are that they are expensive and limits sea access. (3) Revetment rock armour are used as an armor to protect the dune face. The cost is usually lower than solid structures and they have good hydraulic performance and energy dissipation, but as for the sea walls they limit beach access. (4) Offshore structures are structures which purpose is to reduce the wave activity, encouraging the waves to break offshore. When the shoreline wave energy is reduced it encourages sand deposition and the potential for erosion is reduced. The disadvantages for this is that the constructions are usually massive and costly. It can also create navigation hazards, reduce water quality and hinder the natural longshore sand transport by hindering the longshore currents. (5) Sand dunes work as a buffer zone for erosion and both natural and artificial dunes can help to restore post storm damage.

## 3.2 What drives the sand transport?

We now know that erosion and sand transport is what causes the shorelines to retreat. But what drives these processes? As noted from both Short (2020) and Wright, et al. (1979) the wave dominated beach systems can take on many forms depending on the level of energy they experience. And as stated by Aagaard, Greenwood and Hughes (2013), the state the beach system finds itself in decides how the erosion and sand transport will behave. In this section the driving factors for erosion and sand transport will be looked into, and therefore the movement of the ocean around the wave-dominated beaches will be of interest. The three main subjects and their level of impact on beach erosion that will be presented here are waves, rips and tides. Sea level rise will also be brought up, since that can change circumstances in the future.

Rips was shortly described in an earlier section in this report as "What develops when water that's been transported by the waves gets carried back out at sea" (Short, 2020). The rips also get stronger with increasing wave height, as there is more water to be returned seawards. So called beach rips usually reach velocities between 0.5 and 1.5 m/s. This cellular circulation of rip currents is something present at all intermediate beaches. The most common rips are low energy rips. These are located between sand bars and are fixed in their place for the most part. When the waves have not changed in a while, or when the waves are small, low energy rips are most common. When waves increase suddenly, or if a storm is present, high energy or flash rips can form. These tend not to be as stationary as the low energy rips and the flow is faster. There is also a kind of rip that is more permanent. These are called headland rips, fixed rips or topographic rips. These rips develop next to more permanent structures such as jetties and groins. As rips usually flow between sandbars the rips and currents that are not permanent are always changing as the sand and sand bars are always moving with the movement of the water. As the currents of topographic rips are restricted in their movement by the obstacle they usually have a faster flow, often higher than 1.5 m/s (Short, 2020).

More about rip currents and their nature can be found in a study carried out by Aagaard, Greenwood and Nielsen (1997), where "mean currents and sediment transport in a rip channel" was investigated. In this study the main aim was to investigate hydrodynamics and suspended sediment transport in a rip channel along a cross-shore transect, with the main focus on wave energy dissipation and tidal effects while it seeks to identify what factors influence rip flow initiation. They also seek to understand the morphological evolution of the rip channel in response to varying tidal and wave conditions. The result of the study made it possible to draw several conclusions about rips in relation to tides and waves. One important conclusion is that even if the beach is classified as microtidal, tidal effects seem to play a big role in sediment transport and surf zone processes. Rip currents are particularly active during low-tide part of the tide-cycle, and the highest velocities reached at low tide. It is also noted that the rip activity depends on the degree of wave energy dissipation. And lastly, during low tide it seems that offshore-directed rip currents dominate sediment transport, while during high tide the incident waves dominate (Aagaard, Greenwood and Nielsen, 1997).

Short (2020) states the longshore sand transport for the most part takes place in the surf zone, see figure ???. Here the breaking waves suspend the sand which then can be transported by currents. In the case were a beach has a double bar, the maximum transport will happen at the position of the outer bar. This because it's here the waves are the highest. Also, sand transport rates varies

with the wave conditions. Generally, higher waves gives higher sand transport. This especially when the waves are arriving obliquely to the beach, in other words not straight towards the beach. Short (2020) further explains that likelihood of sand transport for a beach will be determined greatly by the degree of its alignment relative the wave direction that is dominant. On the east coast of Australia, which experiences mostly southern waves, the net sand transport will be to the north. Confirmed by both Silva et al. (2012) and King et al. (2021), waves and tides primary controls the net sand transport.

In a paper by Barnes et al. (2011), management and erosion threat of the Sunshine Coast is addressed. They stated that the four key effects waves have on sand transport are the following: (1) When the waves break they generate radiation stresses. Radiation stress is the momentum-flux excess that develops due to the waves presence. This is particularly true in the zone where the waves break where longshore currents driven by the waves may result; (2) The seabed is influenced by the oscillating movement of the ocean waves. The waves generate a shear stress that lifts and suspends the sand on the seabed; (3) The waves in the shallow water are not even, and this results in a noticeable difference in the pressure caused on the sediment bed. The force will be stronger close to the shoreline in the direction the waves travel, which will move the sand towards shore; (4) A bottom return flow will develop in the surf zone due to the waves. The return current will be strongest during storms, in which case they usually overpowers the mass transport and in result move sand offshore.

Lastly, a brief input about sea level rise, since we know that tide has a great impact on erosion and sand transport the sea level rise following the global warming (Leatherman, Zhang, and Douglas, 2000) The connection is highly multiplicative, and it is shown that the long-term shoreline retreat rate reaches approximately 150 times that of sea level rise. This means that a sea level rise of 10 cm could lead to 15 m of shoreline erosion. This is an important thing to keep in mind for future research in the area.

### **3.3 Waves, and their driving forces**

In the previous section the importance of tide, waves, and rips for sediment transport was highlighted. All these factors plays a big part in the sediment transport in their own ways. It is also known that the tide affect both the characteristics of the waves and the rip currents at the same time as the rips and waves influence each other. Although the importance of both tide and rip currents will be kept in mind throughout the following section, the main focus will shift to what influences the size, direction and energy of waves.

So what are the driving forces of Australia's southern east coast waves? The major source of energy that the southern Australian coast is exposed to are the ocean waves (Short, 2020). The tallest and longest-lasting waves originate south of Australia, bringing all of the southern part of the continent a year-round moderate to high southerly swell, with on the most southern part an average height of 5 meters. The waves are at their peak in June through July and at their lowest in November through January. They progressively get shorter as they move north. The waves that reach the east coast originate mostly from the south west and have to refract to reach the coast. This causes them to lose height further and eventually arrive as a southeast swell with an average height of 1.6 m at Sydney, NSW (34°S). Tropical cyclones, east coast lows, and onshore high-pressure winds, particularly northeast sea breezes, all contribute to the creation of additional

waves along the southeast coast (Short, 2020).

The main driving factors of wave conditions deviating from normal conditions are events of storms and cyclones (Short, 2020). In an article by Russell (1993), the mechanisms for beach erosion during storms is investigated. The results suggest that storm events contribute significantly to erosion, especially on high-energy dissipative beaches. An interesting finding in the study is that the erosion is not necessarily connected to the large incident storm waves. Russell found that its the lower frequency motion that is of importance. Particulary the infragravity waves and steady near-bed offshore flows plays an important role in transporting the storm 's impact to the shoreline and inner surf zone. According to Harley et al. (2010), the height of the waves around the Sydney area generally increases and become more easterly during phases of La Nina. See the following section for more on La Niña.

### **3.4 La Niña, Cyclones, and the effects on beach erosion**

We now know that waves influence and drives sand transport and erosion, and we know that storms changes the characteristics of waves making them bigger and stronger. We also know that storms also bring more heavy rain and temporarily risen sea levels which in turn contributes to coastal erosion. In this section the climate oscillation ENSO will be introduced. This since the phase La Niña of the ENSO cycle tends to bring more precipitation and tropical cyclones on the east coast of Australia. A tropical cyclone is a low-pressure system of high intensity that forms over tropical oceans when the water temperature is warm enough to be favorable, at least around 26.5 °C (Short, 2020). The characteristics behind cyclones is that they can develop into very intense storms, and therefore also cause severe erosion.

Beaches along the east coast of Australia have been shown to rapidly erode during La Niña events (Bryant, 1983; Smith, 2001). One of the main reasons are the increasing activity of cyclones, and although these conditions are natural they prove to worsen due to sea level rise causing even bigger waves (Phinn and Hastings, 1992). La Niña events also encourages onshore winds linked to low-pressure systems, leading to increased beach erosion (Smith and Benson, 2001).

El Niño Southern oscillation (ENSO) is a global climate phenomenon which is characterized by the displacement of major weather systems from their normal locations. In an article by Wang and Picaut (2004), the physics behind ENSO is explained. The phenomenon is created due to changes in the atmospheric circulation over the equatorial Pacific area. These changes in circulation are often referred to as a shift in what is called the Southern oscillation. The phases of the Southern oscillation is associated with the tropics of the pacific ocean where the most precipitation is developed and the directions of the trade winds. The trade winds are the constant wind movement towards the equator created by the coriolis effect.

During normal conditions the trade winds blow westwards moving warm surface water along with it. This will cause upwelling of colder water towards the east and America. During normal conditions, the thermocline, which is where the warm mixed surface water and colder deep water meet, will be shallow towards Australia. This since the thermocline in the pacific will not be that steep during normal conditions (Wang and Picaut, 2004). East pacific El Niño occurs when the trade winds in the pacific are weakened or changes direction to western winds instead of eastern. La Niña on the other hand is essentially enhanced 'normal' conditions and occurs when the eastern

trade winds over the pacific become stronger than usual. When the trade winds changes direction during El Niño, warmer seawater is moved east towards north west south America where the water otherwise is relatively cold. At the same time the water around south east asia becomes colder than usual (Wang and Picaut, 2004). During La Niña, when the trade winds are stronger than usual, the warm surface water is pushed away towards Oceania and South East Asia even more than during normal conditions. And at the same time colder water is being pushed up both in the east and the central part of the pacific ocean (Wang and Picaut, 2004).

In parts where the cold water accumulates, dryer weather will occur while more rain activity will occur in the parts where the warmer water accumulates. For Australia, during La Niña, this means more precipitation than usual. La Niña occurs with a frequency of about two to seven years but will last for approximately 1 to 3 years. For El Nino the duration is about 9 to 12 months and occurs on average every two to seven years (Wang and Picaut, 2004).

ENSO and the strength of a La Niña events is measured with the Southern Oscillation Index (SOI) (NOAA Climate, 2023b). This index is a way of measuring atmospheric circulation. The SOI uses the difference in atmospheric pressure between Tahiti and Darwin, but ENSO can also be monitored with the observation of sea surface temperatures. This is done by measuring the temperatures within a region called NINO3.4 which is a region in the central and eastern tropical Pacific, see figure 3.

La Niña and El Niño are not definite conditions. The strength of both La Niña and El Niño can vary, and with that the strength of the consequences. This standard of measure is known as the Oceanic Niño Index (ONI) and a timeseries with values since 1982 is shown in figure 2. In this graph cold phases and warm phases are shown. The typical threshold values for La Niña events are when SIO is sustained above +7 and the temperatures over NINO3.4 are more than  $-0.8^{\circ}\text{C}$  below average. Events are often categorized as moderate to weak or strong depending on how closely they keep their index values to these levels (NOAA Climate, 2023b).

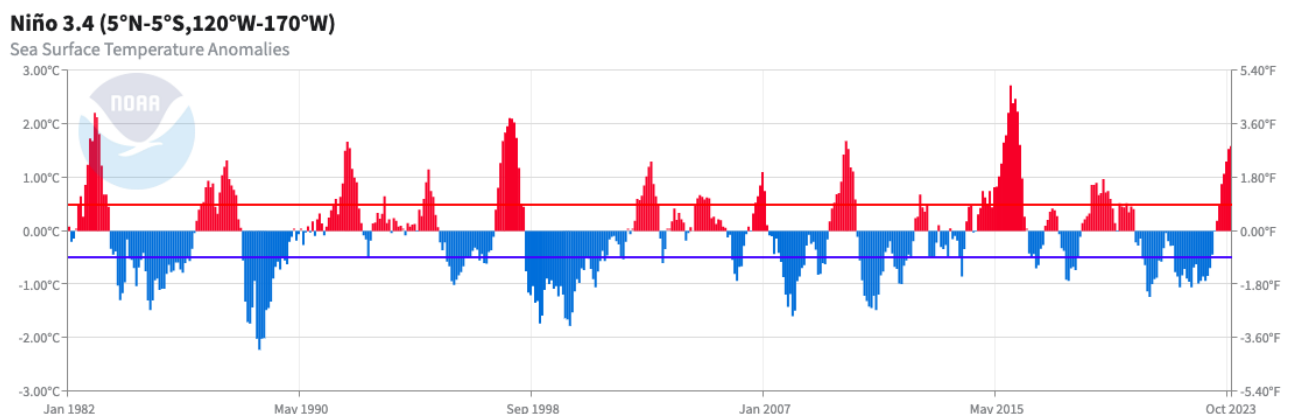


Figure 2: Sea surface temperature anomalies (NOAA Climate 2023b)

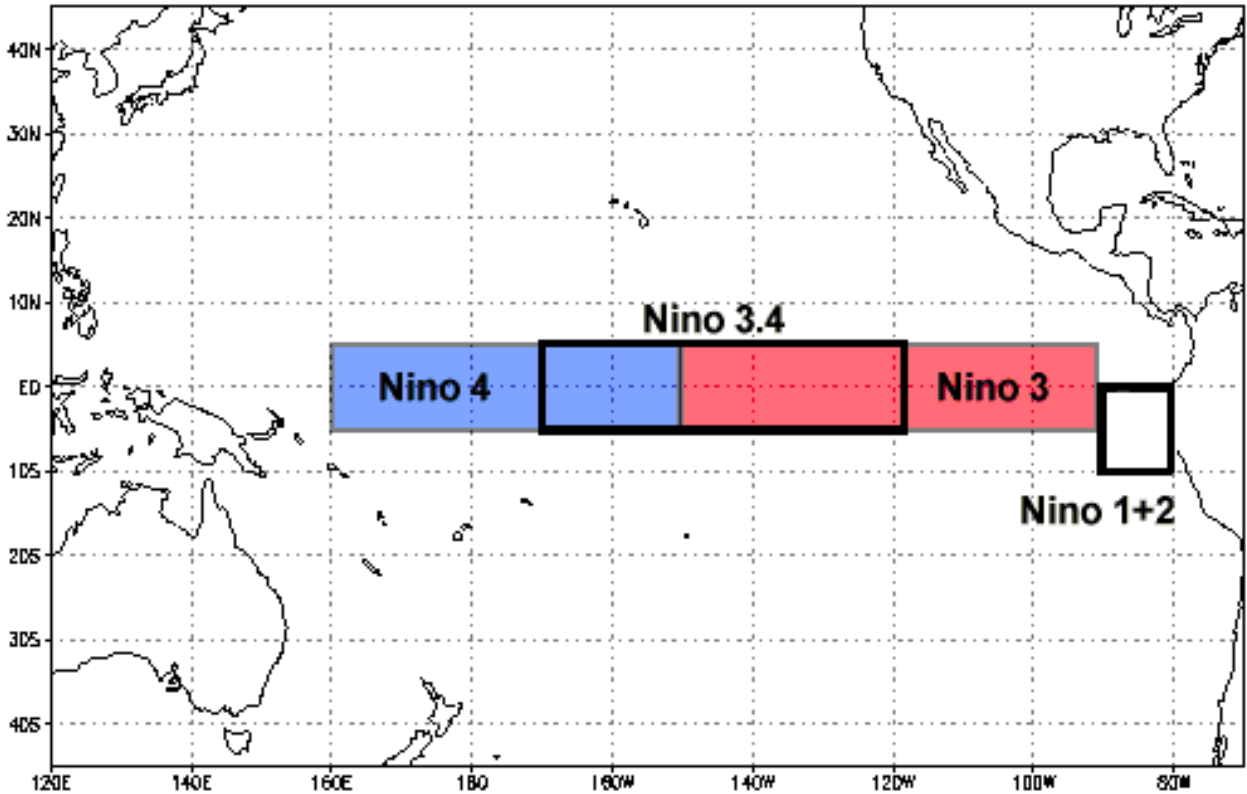


Figure 3: Niño 3.4 region (NOAA Climate 2023b)

In an article by Song et al. (2016), it is shown that during the La Niña period Australia experiences more cloudiness and rainfall than usual, particularly across the north and east part of Australia. The impact of La Niña during the summer is especially detectable for the east coast. The amount of rainfall and the strength of the La Niña event is closely linked, and the greater the temperature difference of the sea surface and the greater the SOI difference from normal conditions, the larger the response in precipitation will be. The frequency and strength of cyclones is also something that tends to increase over the Australian region during a La Niña period. Twice the amount of cyclones make landfall on average during a La Niña year compared to an El Niño year is noted in a report by the Bureau of Meteorology (2016). Landfall is referred to as when the center, or the so-called eye of the cyclone, moves across the coast. During a La Niña year the first cyclone of the season typically makes its debut earlier as well. In the state of Queensland in Australia, located on the east coast, the only years with a multitude of severe tropical cyclones was during La Niña years. With this follows an increased risk of major flooding and damage related to high seas, heavy rain and strong winds (Song et al., 2016).

### 3.5 Coast Snap and citizen collected data

Coast Snap is a beach monitoring program that was established in Sydney, Australia in 2017. It started as a pilot project between the NSW Department of Planning and Environment and the UNSW Water Research Laboratory. The two first sites that it was implemented on was Manly beach and Narrabeen beach, both located on the Northern Beaches of Sydney (Harley and Kinsela, 2022).

The idea behind the program is to involve the community, with the benefits of both raise awareness about the coastal areas for educational purposes and to gather shoreline data in a low-cost way. With a set location and a cradle to position one's smartphone, the data collection is easy to participate in for anyone. At each monitoring site the public is encouraged to take a photo following the simple instructions and submit their contribution to the research and monitoring of the coastline. The photo is then uploaded to the centralized database and can be used as data for various kinds of research (Harley and Kinsela, 2022).

The CoastSnap sites follow an easy design. At each site there is a stainless steel cradle formed to set the smartphone in the right position. The location of the cradle is set to get a good view of the beach at the same time as the location is easily and safely accessed by the public. The cradles are designed to withstand hard weather conditions that the sites often experience, and also potential vandalism. In figure (4), a few examples of how this cradle can look is demonstrated (Harley and Kinsela, 2022). Only location c) Manly, NSW and d) Blacksmiths, NSW is relevant for this report and will be introduced later when the study sites are introduced.



Figure 4: Examples of Coast Snap stations around Australia. a) Wamberal, NSW. b) Lake Cathie, NSW. c) Manly, NSW. d) Blacksmiths, NSW. Pictures from Harley & Kinsela (2022).

Next to the cradle a sign is implemented with instructions for members of the public that want to be contributors and participate in the CoastSnap program. In figure (5) an example of such a sign can be seen. The steps for the public to participate are easy. Firstly the smartphone is placed in the cradle in the correct position. Secondly a picture is taken, making sure no special features are on, like the zoom function or a filter. Thirdly the image is submitted to CoastSnap. This can be done in several ways, for example through facebook or twitter, and in the latest years through CoastSnaps own phone application that makes the process of submitting the image very easy. The submitted photos are later added to the centralized database making them accessible for analysis (Harley and Kinsela, 2022) .



Figure 5: Example of CoastSnap signage. Image from Harley & Kinsela (2022).

After a while the combined photos submitted from the same angle and same position form a valuable set of data. One important and useful form of data the images can generate is the position of the shoreline, and with a set of data the change in position over time. The process of using images in this way is known as photogrammetry. The first part in the process of determining the position of the shoreline is to connect the pixels in the photograph with real world coordinates. This takes the photos from the raw form to a georectified “birds-eye view” format. To connect the picture to world coordinates a GPS survey has to be done. In this survey, so called ground controls points are created. The points are objects that can be seen in the image and these points and their GPS coordinates makes it possible to relate the image to a x,y,z coordinate system and makes the rectifying of the image possible (Harley and Kinsela, 2022).

An algorithm later distinguishes the difference in color of the sea and the shore and with that the shoreline can be automatically detected. The tide changes and has to be taken into account of course to get true data. This is done by using the timestamp of the submitted images and correcting the tide using the local time and wave data. When the process of mapping the shoreline is repeated for suitable images, useful information of the shoreline position change over time can be gathered (Harley and Kinsela, 2022).

The idea and implementation of collecting the images is easy, but behind the processing that follows, shortly described in this section, are advanced image processing algorithms that make it

possible to determine the shoreline position. A lot of the algorithms used in this report to process the images to data are already established and well used by those who are involved with research based on coast snap images. These steps and algorithms will be more thoroughly described in the method section of this report.

### 3.5.1 Data

One of the issues with citizen collected data is that the frequency of the data can't be controlled in the same way as with field data for example. It is therefore of interest for this study to have an idea of the frequency of the data collected in similar studies. In a study by Liu, et al. (2013), satellite images were used to detect coastline change. In this study 32 sets of Landsat-MSS/-TM-ETM+ satellite images were used over the period 1973-2009. That is 32 images over the span of 36 years, resulting in 0.89 images per year. In another study by Deburghraeve, et al. (2023), 65 CoastSnap images over a 9 month period were used. This is considered a high frequency dataset. In another report by Elrick-Barr, et al. (2023), CoastSnap images was also used with the aim to understand coastal social values through citizen data. During the period between mid-December 2021 to mid-July 2022, 95 complete survey responses were submitted which was for 3 different locations combined. 43% were used in the next process of analyzing the data. That leaves approximately 41 images left for analysis. This means that over the time period of 7 months, 5.9 images per month were available for analysis. This divided by the 3 locations gives approximately 2 images per month on average per beach.

Monitoring the coastline frequently is crucial for management decisions to be effective (Smith and Benson, 2001). For long term research, the monitoring have to be extensive enough that the Pacific-wide El Niño-Southern Oscillation fluctuations and seasonal shifts can be captured by the data. This includes conducting repeated and regular surveys over long periods of time. If the potential long term effects of ENSO is of interest, data samples needs to be present for both the La Niña and El Niño periods. This since the potential erosion as a consequence of La Niña can be reversed during a following El Niño period (Smith and Benson, 2001). In combination with this, the beach monitoring needs to be done at a monthly interval this to "enable a representative sample of natural beach change to be measured". To have enough data for effective management decisions to be taken, some key sites might have to have maintained monthly beach monitoring for all time. For areas that are less sensitive to beach erosion data can be collected less frequently (Smith and Benson, 2001).

## 3.6 Shoreline modeling

As previously mentioned, sandy coastlines are dynamic and complex environments that are constantly changing under the influence of natural and human factors. Coastal communities face threats such as erosion and flooding, which can have devastating consequences for both people and the environment. Being able to predict shoreline changes is therefore of great significance for the sustainability of coastal communities, as it helps with inventing strategies to protect coastal areas from damage in the future. In addition, with the increased sea levels as a consequence of climate change, chances are extreme weather conditions becoming magnified and more frequent which can have a dramatic impact on the coastline. Therefore, one of the biggest challenges and drivers for research in coastal research is to develop tools that can be used to quantify the possible impacts

along sandy coasts in response to future climate change.

### 3.6.1 Empirical equilibrium cross-shore models

One of the most common approaches for prediction shoreline position on sandy coastal areas are empirical cross-shore models. These models operate by utilizing coefficients that are calibrated with previously observed data (Splinter, et al., 2014). This approach is the most effective for predicting shoreline changes involving longer time scales (seasonal to decades or more) as well as larger spatial domains, from a single beach to an entire region (Davidson, et al., 2013; Miller and Dean, 2004; Yates, et al., 2009). As the general name for this type of model reveals, empirical cross-shore models are specifically aimed at predicting shoreline changes along the vertical (cross-shore) axis, i.e. how the shoreline moves closer or further away from the sea over time. This does not necessarily mean that longshore sediment transport is neglected, as it may be included in the model if it is considered a relevant factor for shoreline change at a specific location (Hanson, 1989; Nam et al., 2011).

An example of one of the earlier empirical equilibrium cross-shore models is the Dean model, also known as the Dean Beach Erosion Model, which was developed by the engineer Robert A. Dean (Dean, 1977). The Dean model has been an important point of reference in the field and has contributed to better understanding of the complex relationship between waves, sediments and shoreline processes. Dean coined the theory of the equilibrium beach profile, which explains that for a given wave energy there is a corresponding equilibrium profile where the wave energy does not generate any morphological change on the beach profile. The size of the wave energy in relation to the equilibrium energy thus leads to an adaptation of the beach profile. This results in a function of both the current state of the beach profile and the difference between the equilibrium wave energy and the incoming wave energy.

Later on, the disequilibrium concept was introduced by Wright, et al. (1985). It is a theoretical model that explains the relationship between shoreline changes and dimensionless fall rates. The concept is based on the Dean number  $\Omega$ :

$$\Omega = \frac{H_b}{Tw_s} \quad (1)$$

where  $H_b$  is the wave height at the breaking point,  $T$  is the wave period and  $w_s$  is the fall velocity of sediment particles. The dean number describes the shape of the beach profile, indicating that the beach profile is reflective with a steep slope when  $\Omega < 1$ , and dissipative with less slope when  $\Omega > 1$ .

Wright, et al. (1985) noted that there is a disequilibrium between the current fall rate  $\Omega$  and the equilibrium rate  $\Omega_{eq}$ , which is defined as a function of the weighted mean of the preceding dimensionless fall rate. It was concluded that the beach will move in opposite directions depending on whether  $\Omega$  or  $\Omega_{eq}$  is greater. The disparity arises due to past morphodynamic and hydrodynamic conditions, which were found to be strongly linked to future morphological conditions. In summary, the disequilibrium concept is a way of describing how both past and current coastal environmental conditions affect sediment transport and thus changes in the beach profile.

Inspired by the past progressions in shoreline modeling and coastal research, today's models have evolved into more advanced empirical models including more complex processes and a wider range

of parameters and factors taken into account. In addition, advances in computer-aided technology and increased data availability have provided the models with better conditions for making more precise and reliable forecasts. This has laid the foundation for the empirical equilibrium cross-shore model ShoreFor, which is the model used for the calibrations in this report.

### 3.6.2 The ShoreFor model

The first version of the ShoreFor model was presented as a two-dimensional profile model in Davidson and Turner (2009), simplified in Davidson, et al. (2010) and improved in Davidson, et al. (2013). In the latest adaptation the development, calibration and verification of the resulting one-dimensional behavioral coastal forecasting model is described, which primarily includes the displacement of the shoreline due to the influence of wave-driven cross-shore sediment transport. The model uses a dynamic equilibrium condition that develops over time with the weighted previous dimensionless fall velocity.

The equation governing the model is known as a relaxation equation. This equation describes the manner in which disturbances impact the beach and subsequently return to a state of equilibrium, and is presented in the following form:

$$\frac{dx}{dt} = b + \frac{c^{\pm}}{P^{\frac{1}{2}}}(\Omega_{eq}(t) - \Omega(t)) \quad (2)$$

where  $dx/dt$  is the rate of change of shoreline position ( $x$ ) with respect to time,  $P$  is the incident wave power (calculated with linear wave theory) and  $c^{\pm}$  are two free parameters that define erosion or accretion rates.  $c$  depends on the sign of the equilibrium ( $\Omega_{eq} - \Omega$ ), which according to Yates, et. al (2009) means that  $c$  is separated into erosion if negative, and accretion if positive.  $b$  is a component that is independent of wave action and reports the trend in the shoreline affected by processes that have not yet been taken into account. The inequilibrium term ( $\Omega_{eq}(t) - \Omega(t)$ ) was for the first time introduced as a time-varying equilibrium condition, based on the imbalance concept of Wright, et al. (1985), which appeared to contribute to significant improvements for prediction of shoreline change for multi-year time periods (Davidson, et al., 2013).

The resulting ShoreFor model proves to be a simple but effective tool for predicting shoreline changes in response to variations in sediment supply and sea level rise. It has demonstrated an impressive ability to forecast shoreline position and beach width along sandy coasts over time, as well as changes in beach volume and sediment transport, taking into account complex factors including energy balance, wave conditions and antecedent conditions (Davidson, et al., 2013).

## 4 Study sites

7 different study sites are used for this study, all located on the southern half of the Australian East Coast. The locations of each site are illustrated in figure 1. A short observation on each location based on satellite-maps and images will be presented. This since the area of the beach and it's geographic location is a contributed factor in sand movement which is of importance for the cause of erosion. For some of the locations, further information about the current state and

existing coastal monitoring could be found, and therefore this will also be brought up in the following section as it might serve a purpose in the later discussion.

#### 4.1 Alexandra Headland beach

Alexandra headland beach is located approximately 100 km north of Brisbane and stretches a distance of approximately 500 metres. The Coast Snap station is located on the south part of the beach pointing north, see figure (6).

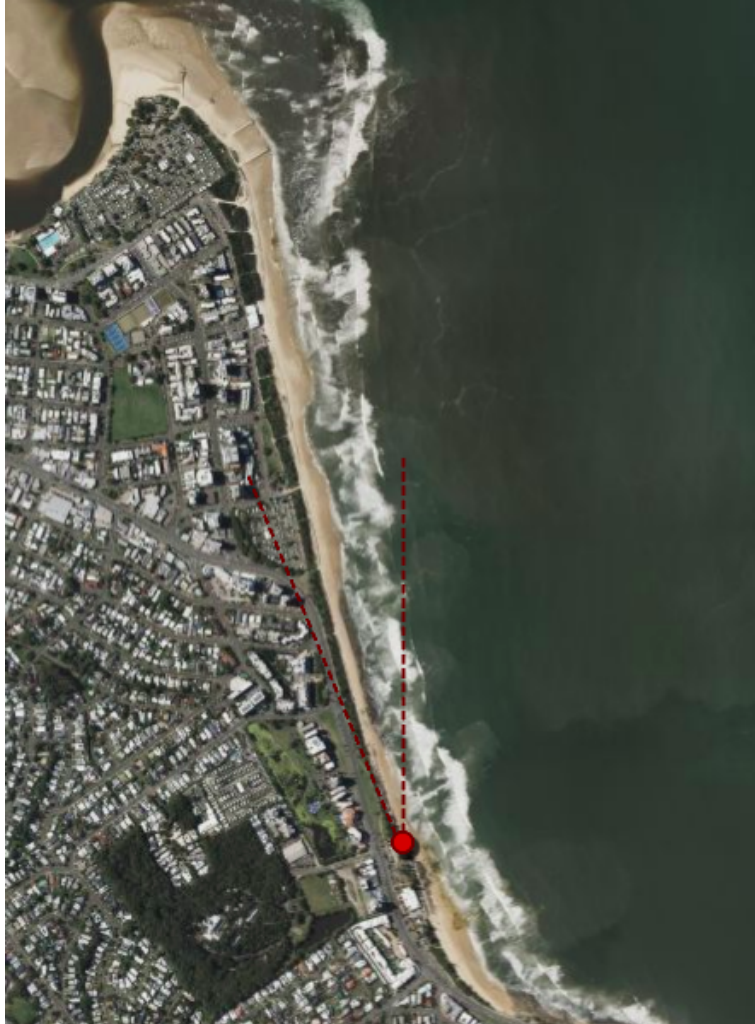


Figure 6: Top part of image facing north. Satellite image of Alexandra Headland Beach where the location and direction of the CoastSnap station is shown (Apple maps 2023).



Figure 7: Alexandraandra Headland Beach from Coast Snap station 2021-12-19 (Coast Snap data base 2023).

## 4.2 Buddina Beach

Buddina Beach is located slightly south of Alexandra Headland Beach, with a headland separating them with Buddina located south of it. The cost snap station for Buddina is located at the most north end of the Beach pointing south, see figure (8).

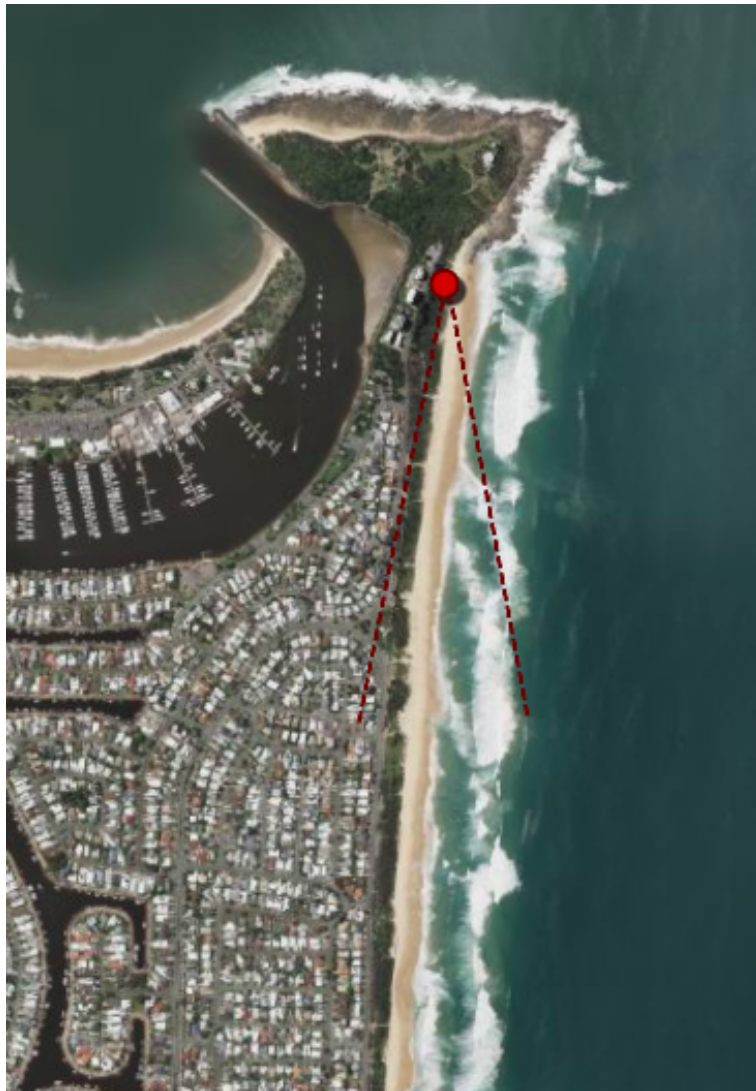


Figure 8: Top part of image facing north. Satellite image of Buddina Beach were the location and direction of the CoastSnap station is shown (Apple maps 2023).



Figure 9: Buddina Beach from Coast Snap station 2021-11-25 (Coast Snap data base 2023).

### 4.3 Stockton Beach

Stockton beach is located on the north side of a break wall. The beach is more than 30 km long and is embossed with large sand dunes. At some locations the beach reaches a width of almost 1 km, but at the far south end, where the CoastSnap station is located (see figure (10)), the beach is at its narrowest and has no dunes. Houses in the area are built very close to the beach and are exposed to a risk of damage in cases of storms, storm surges and high wave conditions. Sand mining is also something practised at Stockton beach, which has led to a loss in vegetation over time according to the City of Newcastle (2020). The Newcastle Harbour prevents sand from coming in from beaches to the south, and with significant longshore transport to the north but no new sand coming in from the south Stockton Beach is at large risk of erosion.



Figure 10: Top part of image facing north. Satellite image of Stockton Beach where the location and direction of the CoastSnap station is shown (Apple maps 2023).



Figure 11: Stockton Beach from Coast Snap station 2020-02-04 (Coast Snap data base 2023).

#### 4.4 Blacksmiths Beach

Blacksmiths beach is almost 15 km long and at the South end of the beach the Swansea Channel enters. Here a breakwall is placed acting like a border between the beach and the channel (NSW Government, 2023b).

The beach is a popular surfing spot and according to Drummond, et al. (2020), its frequent visitors have noticed a change in the surf. They have noticed that fewer surf breaks are present and that the profile of the sand under the water has become steeper which has resulted in more of a shore break, meaning the waves are breaking close to the shoreline. A change of the dunes have also been observed. The sand dunes act as a protection from storm erosion, coastal recession, wave run-up and future sea level rise on settlement near shore. The change in the dunes makes the area more vulnerable to future storm events and sea level rise. Also, several medium trend cycles has been observed at the site, which appear to have some correlation to ENSO (Drummond, et al.,

2020).

The CoastSnap station is located on the far south side of the beach at the start of the Break wall, shown in figure (12).

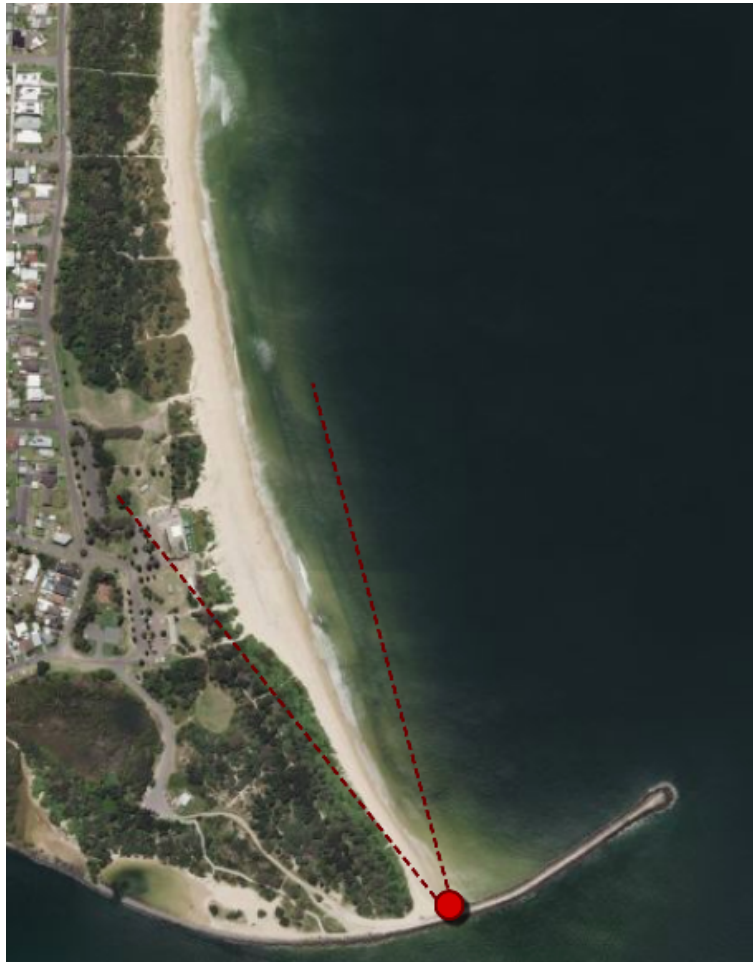


Figure 12: Top part of image facing north. Satellite image of Blackmiths Beach were the location and direction of the CoastSnap station is shown (Apple maps 2023).



Figure 13: Blacksmiths Beach from Coast Snap station 2020-05-06 (Coast Snap data base 2023).

## 4.5 North Narrabeen Beach

Figure (14) shows the location of the North Narrabeen CoastSnap station. The cradle is located on the north part of the beach and is pointed north. The North Narrabeen beach is located in the northern Sydney area in the suburbs of Northern beaches. The beach is over 3 km long. In the north end a lagoon entrance is present. The beach faces east and is protected to the south by a 36-meter-high Long Reef Point that extends two kilometers into the sea (Sydney, 2023).

North Narrabeen beach has a long history of beach monitoring and is well documented even before Coast snap. Since April 1979, according to the Narrabeen Collaroy Beach Survey Program (UNSW 2023), a beach profile survey program has been done monthly. This monitoring is unique since long-term datasets of these kind on sandy beaches are rare.



Figure 14: Top part of image facing north. Satellite image of North Narrabeen Beach where the location and direction of the CoastSnap station is shown (Apple maps 2023).



Figure 15: North Narrabeen Beach from Coast Snap station 2020-01-04 (Coast Snap data base 2023).

## 4.6 Manly beach

Manly beach is located on the northern beaches north of Sydney in New south wales, facing the southeast coast of Australia. The beach curves 1.5 km in total, including North Steyne and Queenscliff that are parts of the same shoreline, but carries different names. In figure (16), the position of the CoastSnap station can be seen. The cradle is located on the southern part of the beach and is pointing north.



Figure 16: Top part of image facing north. Satellite image of Manly Beach where the location and direction of the CoastSnap station is shown (Apple maps 2023).



Figure 17: Satellite image of Manly Beach, zoomed out (Apple maps 2023).

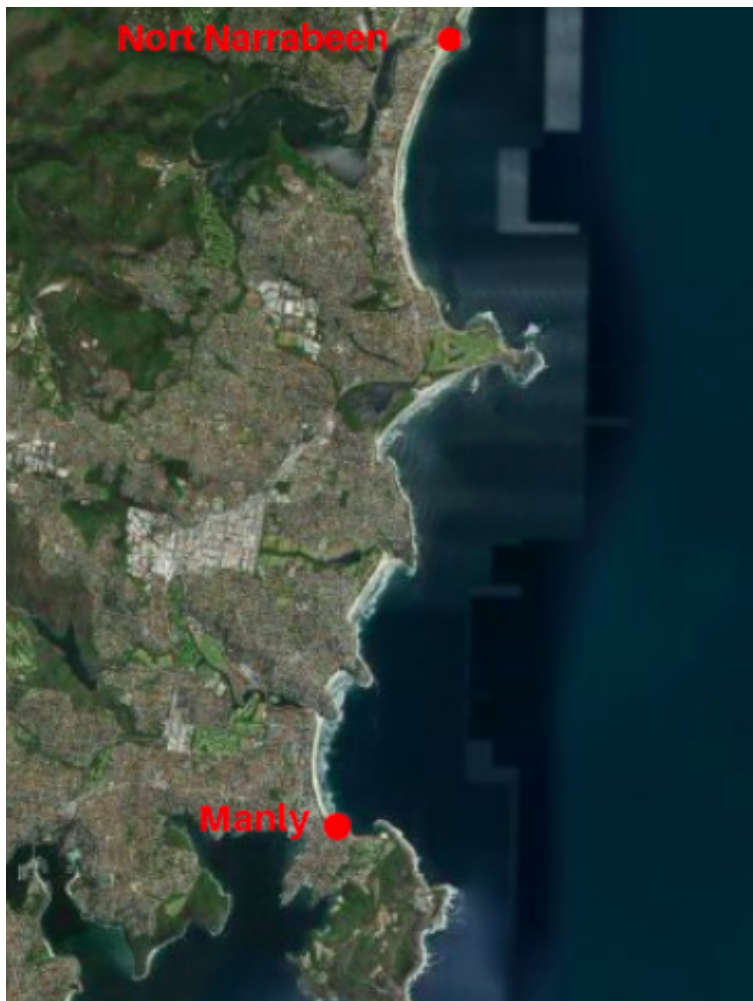


Figure 18: Satellite image of Manly Beach and North Narrabeen Beach, with their CoastSnap stations marked (Apple maps 2023).



Figure 19: Manly Beach from Coast Snap station 2020-01-01 (Coast Snap data base 2023).

## 4.7 Broulee Beach

The Broulee CoastSnap station is located on the northeast headland and is pointing in a southwest direction, figure (20).



Figure 20: Satellite image of Broulee Beach where the location and direction of the CoastSnap station is shown (Apple maps 2023).



Figure 21: Broulee Beach from Coast Snap station 2020-02-24 (Coast Snap data base 2023).

## 5 Methodology

In this section, the Methodology on how this study was executed will be presented. It is divided into two parts in the same manner as the section about the research questions (see 2.2, as this study holds two main parts; 1) Impacts of La Niña and 2) Shoreline modeling. Before this distinction, a general part of the methodology which is common to both parts is described.

### 5.1 General

The first part of the method referred to as "general" is the process of mapping the shorelines. This process was done for all the sites and is the foundation to all the data used in this project. The Raw data used for both parts of the projects were images from CoastSnap from 7 different official CoastSnap sites.

### 5.1.1 Collecting of Images

The process of collecting CoastSnap images and mapping shorelines is described in the report “Shoreline change mapping using crowd-sourced smartphone images” (Harley, et al., 2019), which is the same methodology for processing data in this study.

#### Collecting the images

At each study site used in this study, a stationary stainless steel cradle is found. This is where citizens who want to participate in the CoastSnap project place their smartphone to snap a photo. Examples of cradles is shown in figure (4). The cradle is used to constrain the position of the camera as well as azimuth, tilt and roll of the images. Following seven study sites are used to answer the research questions for part 1), listed from north to south; Alexandraandra Headland Beach, Bud-dina Beach, Stockton Beach, Blacksmiths Beach, North Narrabeen Beach, Manly Beach, Broulee Beach. In part 2), data from Manly beach only was utilized.

After the images are shared by the community they are uploaded to a centralized database. The way the images used in the study have been collected varies. In the study by Harley, et al. (2019) it was stated that a variety of options for submitting the images is available, including Facebook, e-mail and hashtags on twitter and instagram. The more previous images used in this study have most likely been uploaded straight to the Coast Snap smartphone application. In this study the images were directly downloaded from the centralized database where all the images from the CoastSnap sites are stored. The amount of images submitted from the different locations investigated in this study varies greatly, where Manly and North Narrabeen are the two more well documented sites.

### 5.1.2 Shoreline change and mapping

When this project started all of the locations in this study were existing sites. This means that its listed as an official site in the CoastSnap data base and ground control points are usually already made. Because of this the images could be downloaded from the centralized database and the shorelines easily mapped with the pre existing matlab algorithms created by Dr. Mitchell Harley (Harley et al., 2019).

The method used for mapping the shorelines is a process divided into three steps; creating ground control points, rectifying the image and lastly mapping the shoreline.

#### Creating ground control points

When the image has been processed and put into the centralized database, the image now has to be georectified. This means that the picture is matched with world coordinates. This is done by manually choosing a series of objects that are visible in the image and using them as fixed ground control points (GCPs). The ground control points are usually measured when the new CoastSnap site is created.

For all of the sites in this study the, GCPs were already made. However, GCPs were implemented for one specific site called Queenscliff beach. Queenscliff was intended to be used in the study but ended up not being included since its practically the same beach as Manly beach (that is already

included in this research) only pointed in the other direction (the north end of the beach). Since the GCPs for Queenscliff beach was implemented before this was decided, it will serve as a demonstration since this is the method that has been used for all the other beached included in the study.

The first part in the process of creating the GCPs is to choose the locations of the GCPs. This is done by looking at one of the images taken from the picture location and deciding where good ground control points could be located. For Queenscliff, 8 GCPs were chosen from one of the existing images. The locations that are chosen for GCPs are stationary objects that will remain and be easily visible in all pictures, like buildings for example.



Figure 22: Picture of Queenscliff beach with the chosen ground control points marked.

Once the location of the picture location/cradle as well as the GCP locations are specified, a GPS survey is executed. This was done with an RTK-GPS. The RTK-GPS is used to get extremely accurate GPS points. RTK stands for real time kinematics, and different from just receiving a normal signal from the Global Navigation Satellite Systems, it also takes correction stream into account. This will give the measurements an accuracy of 1 cm. In this particular case there was no cradle installed since this was a newly opened site and not yet official, it was a so-called "do it yourself" site. But a pole of a fence was specified where the image should be taken, which was

where the coordinates were measured for the picture location. All the coordinates are in a in a  $x$ - $y$ - $z$  field, where the height in in the  $z$  direction also measured with the RTK-GPS.



(a) Picture location measured at Queenscliff beach



(b) Measuring GCP 2 at Queenscliff Beach.

Figure 23: Pictures from GPS survey

The coordinates for the GCPs are then put into an excel spreadsheet where all the data of the different locations are stored. The existing code that is being used in Matlab for the later steps is loading this information from the excel-file.

### Rectifying images

Image georectification is the process of transforming the image from existing on a plane with pixel coordinates  $(U, V)$  to world coordinates  $(x, y, z)$ . The world coordinates are divided into; northings, eastings and height. The northing and easting describes a point geographically in a Cartesian coordinate system. The northing is the distance measured northward and is represented by the  $y$ -coordinate and the easting is distance measured eastward and is represented by the  $x$ -coordinate. The height is represented by the  $z$ -coordinate. To do this transformation a simple pinhole camera model is assumed using a homogeneous formulation. The pinhole camera model defines the mathematical connection between the position of a point in three-dimensional space and its corresponding projection onto the image plane of an idealized pinhole camera. In this model, the camera aperture is represented as a single point, and there are no lenses involved to focus the light (Harley et al., 2019).

Practically, in the matlab program this is done by running the codes and then loading the image of choice. The following step that rectifies the image is done by pointing out the GCPs in the picture. Since the world coordinates of the GCPs are known it can then distort the image to a

bird's-eye view.

### **Shoreline mapping**

When the image has been georectified, the next step is to map the shoreline. This means that we want to know the exact position of the shoreline in world coordinates. To do this the shoreline in the rectified images gets defined as where the “wet” and “dry” pixels meet. The wet pixels represent the ocean surface and the dry pixels represent the beach sediments. This can be done with several different methods, but the method used in this study is done by detecting the difference in the red and blue colour channels (RmB colour space). By doing this the shoreline can be detected automatically and does not have to be “drawn” manually. Although in some cases the RmB were not as favorable and the shoreline had to be edited manually to follow the exact ocean edge. This might be the case in foggy weather or later at night where the colors in the picture are washed out, and the reds and blues are hard to detect.

Red minus Blue (RmB) color space samples are taken using transect files, which are predetermined cross-shore transects that span the beach and surf zone. The best threshold RmBOPT (red dashed line) for shoreline detection is then determined using the resulting image-wide bimodal distribution. The transect files were already made for all of the beaches used to hypostasis in this study, with an exception for Queenscliff where new transect files were made. But as previously stated, Queenscliff ended up not being included in the study.

### **Tidal correction**

Since the tide differs in elevation over time the tide has to be corrected in some way to get a correct result. The approach taken is the same as in the 2019 report by Harley, et al. (2019). An elevation  $Z(sl)$  is calculated which is determined by the model:

$$Z(sl) = Z(tide) + \Delta Z(constant)$$

$Z(sl)$  is the assumed constant elevation alongshore, and  $Z(tide)$  is the position of tide at the time when the picture was taken.  $\Delta Z(constant)$  is a constant that takes characteristic of the particular shoreline into account.

This is a simple but effective approach. But because of the simplicity of the model it is important to note that large errors could occur if the images are taken and used during unfavorable conditions. These conditions are mostly during storms when the tidal anomalies and/or offshore waves can occur and be significant. But these errors are reduced due to the fact that images are very seldom collected during extreme conditions like this.

## **5.2 Part 1: Impacts of La Niña**

Here the methodology for part 1 will be presented. This is the methodology for answering if the data shows what the literature implies, which is that La Niña should have eroded the shorelines of the east coast, as well as investigating if the quantity and quality of the data is enough to do quality research.

### 5.2.1 Time frame

To answer hypothesis 1 a period of the last la Niña event had to be defined. From figure (2) the last La Niña event can be defined. The most recent negative period is according to this graph is between May 2020 and March 2023. And since the start of this project took place at the end of January 2023 the timeframe chosen for this project were decided to be 1 January 2020 - 1 February 2023.

### 5.2.2 Choosing a site

To further investigate hypothesis 1, 7 different beaches listed in section () along the east coast of Australia were investigated. The beaches were chosen on three bases.

1. Existing site
2. Sufficient data
3. Quality of data

First of all, beaches that already had an existing Coast Snap station were prioritized. And all the Beaches that ended up being investigated in the end were pre-existing Coast Snap stations. Secondly, locations where data was not sufficient were ruled out. The goal was to have at least one image per month for the period 1 Jan 2020 - 2 Feb 2023. Very few of the locations fulfilled the requirement of the length of the time period. It was decided that there should be existing data for more than a year at least. But the requirement for at least one image per month is fairly consistent throughout the chosen beaches, with the exception of a few gaps that were assessed to be sufficiently insignificant to the end result to be included anyways. Thirdly the quality of the pictures were investigated. For some of the locations that were ruled out there were different problems with the processing of the pictures, or there was something wrong with the GCPs for the site. To get a good result as stated previously the pictures have to be of good quality and the colors can't be washed out or muted. Also the pictures have to have been taken in the right spot from the right angles.

### 5.2.3 Data selection

Once the locations were chosen shorelines were mapped for at least one image per month, and approximately two per month if the amount of images allowed it. Shorelines might be mapped for more images if a very clear storm event were present. Pictures for the time series that are during storms will be avoided. But pictures right before and right after will be prioritized. This is as mentioned before because pictures during the storm give a faulty indication of where the shoreline sits. But pictures right before and right after show how the shoreline has changed during the storm.

All the data was also plotted in a combined graph with the only purpose to show which date all the data used is from. This to visualize how much data that is used for the different locations and pinpoint if there is a gap that turns out to be of significant value for the results.

Tidal allowance is set to 0.2 m for all locations besides Alexandraandra Headland Beach which is set to 0.5 m to get sufficient amount of data. The tidal allowance is how much the tide at the time of the different pictures used as data is allowed to differ in an interval. 0.2 tidal allowance

means the tide from the starting picture is allowed to range between  $\pm 0.2$  m from the starting tide.

To visualize the data distribution of the used data a graph was made where the data was shown as dots on a time-line, figure 39. This to get a better grasp on the distribution. By visualizing this, data gaps and hot-spots can be more easily spotted, as well as comparing the distribution of data between the 7 different study sites. It was also noted how many images that were available for the investigated period in contrast to the amount of images used from the time-series. The amount of pictures used were also divided by the time period for each site to get an average quantity of images per month used. This is summarized in a table 7.

#### 5.2.4 Timeseries

The data from the mapped shorelines were then plotted alongside the wave data for the same period. The wave data used is from the Sydney waverider buoy which is collected by the Manly Hydraulics Laboratory. The data that's downloaded from the mapping of the shorelines in Matlab contains both the raw beach width and the smooth beach width. They both refer to the average width of the beach but the smooth data is the average after the shoreline has been smoothed out. Both the raw and smooth data is plotted in a graph. For the smooth data a line is connected but the raw data is just shown as data points. The wave data is presented in a graph directly under the beach width data, with the same timeline and scale. The annual-trend was calculated for each time series by calculating a linear regression taking all points into account. From this linear regression an annual trend in beach width change could be calculated. It is this trend that is presented in each graph and referred to as annual trend. An end-point result was also added to each graph with timeseries. This is the difference between the first data point and the last for each timeseries.

To evaluate the adequacy of the linear model, the coefficient of determination ( $R^2$ ) was computed. This statistic represents the proportion of variance in the dependent variable (beach width) that is predictable from the independent variable (time). An  $R^2$  value close to 1 suggests that the model explains a large proportion of the variance, indicating a good fit. Conversely, an  $R^2$  value near 0 implies that the model does not adequately capture the data's variability. The residuals, or differences between the observed beach widths and those predicted by the linear model, were squared and summed to obtain the residual sum of squares. The total sum of squares, which measures the total variance in the beach width data, was also calculated. The  $R^2$  value was then derived using the formula  $R^2 = 1 - (\text{residual sum of squares} / \text{The total sum of squares})$ . The  $R^2$  value obtained from the analysis was annotated onto the plot in a textbox, providing an immediate visual indication of the model's fit.

To assess the hypothesized relationship between beach width and wave height, where a decrease in beach width is expected to correlate with an increase in wave height, a linear regression analysis was conducted using time-series data from both the beach width and the wave height. To temporally align the two datasets, the wave height data were interpolated to match the dates of the beach width measurements using MATLAB's `interp1` function with a linear method. This ensured that each wave height data point corresponded to a beach width measurement on the same date, which is critical for accurate correlation analysis. A linear regression was selected to model the potential linear relationship between the two variables, hypothesizing that higher waves might contribute to greater beach erosion, as reflected in a reduced beach width. The lin-

ear model was defined in MATLAB using the `fitype` function with 'poly1', representing a simple linear relationship of the form  $y = a * x + b$ . The model was then fitted to the interpolated wave height data (independent variable) and the normalized beach width data (dependent variable) using the `fit` function. The fitting process produced a best-fit line that represents the estimated linear relationship between wave height and beach width. To visualize this relationship, a scatter plot of the observed data was generated and overlaid with the linear fit line. Additionally, the  $R^2$  value was included in the legend of the graph to provide a quantitative measure of the goodness of fit, indicating the proportion of variance in the beach width that is explained by the wave height.

The results from the timeseries was also combined into a bar chart to visualize the difference in erosion for the different locations. An average for all the beaches, both for annual trend and end-point was also calculated and added as lines. The averages was calculated as mean-values.

### 5.3 Part 2: Shoreline modeling

Local communities are wanting to know more about their coastline and be able to understand/predict how beaches may change into the future. The most used tool for calibration and hindcasting shoreline position changes is empirical cross-shore models. Application of these models require high quality local observations of both the beach, as well as the forcing conditions that drive beach change to adjust the free parameters of the model.

A freely available version of ShoreFor (ShoreFor v1.0) will be used for all modeling scenarios in this study. The model requires one set of shoreline data (morphology observations) and one set of wave data (forcing data). Morphology observations with an adequate amount of data points and of sufficient quality can be both hard and expensive to come by. Forcing data is globally available as wave data retrieved from buoys far from shore, however, the ideal is to have high quality inshore wave data but it is much harder to come by.

As new community-based methods for coastal monitoring that utilise smart phones are readily available for anyone to contribute to coastal monitoring, such as CoastSnap, this study explores how well citizen supplied beach data (morphology observations) can be used to train a cross-shore equilibrium model. The model performance was tested by degrading the original set of CoastSnap data, both in calibration length and sampling magnitude, and in using inshore vs offshore wave data. This inquiry was divided into two key questions;

- 1) How much data from CoastSnap is needed to train ShoreFor v1.0?
- 2) Is inshore/local wave conditions needed in order to get good model results when training the ShoreFor model with CoastSnap data?

#### 5.3.1 Data generation

The ShoreFor model requires 2 sets of inputs - morphology observations and forcing observations. The morphology data is the responsible variable for the modeling, in this case the shoreline data. The forcing observations is the independent variable that drives the shoreline change, in this case wave data.

#### Morphology observations

All modeling scenarios with the ShoreFor was executed with shoreline data generated from one of the CoastSnap stations. The ideal is to have as many data points as possible. Therefore Manly beach was chosen as the study site for this purpose, as it is one of the sites where the community has shown most interest in contributing and also provides the longest duration data set. The shoreline time-series spans from May 17, 2017 to February 20, 2023 and consists of 1227 images with intermittent frequency. The images was mapped and transformed into data as described in chapter 5. The observed morphology data includes the following:

Table 1: Morphology observation data

Variable	Definition
Shoreline x(t)	Timeseries of the shoreline position (x)
Dates	The dates associated with the measured shoreline position
Elevation	Elevation of the sea level (metres)
Std	"Shoreline measurement Standard Deviation" = horizontal fluctuations between the shoreline and transect intersection points (metres)

### Forcing observations

The forcing data was retrieved from ERA5 by the European Centre for Medium-Range Weather Forecasts (ECMWF). ERA5 is a global dataset containing information about various weather parameters such as temperatures, winds, precipitation, humidity, waves and more. The wave data that was used for calibrating the ShoreFor model was retrieved from a buoys located offshore (COORDINATES?) off Sydney. The data and spans from January 1, 1979 to December 31, 2022 and is evenly spaced with an hourly frequency. Since the model only needs a forcing timeseries of 5 years prior to the shoreline timeseries for executing calibrations, the dataset was shortened by removing all the datapoints up to 2010. The forcing data includes the following:

Table 2: Forcing observation data

Variable	Definition
Hs	Significant wave height (metres)
Tp	Peak wave period (seconds)
Dates	Dates associated with the measured wave data
WaveDir	Average wave direction

### **Creating inshore wave conditions**

As the wave data from era 5 is retrieved as offshore parametric wave data far from the CoastSnap station located near the shoreline where the shoreline data is retrieved, a matlab script called MIKE21 Spectral Wave (SW) was used to dynamically transform the offshore wave scenarios to nearshore parametric wave data. MIKE21 SW is a phase-averaged spectral wind-wave model that computes random short-range wind-waves for coastal and inland areas (Mortlock, 2014). It is a third generation wave model, meaning it is advanced enough to take several sets of wave phenomena into account, such as the direction of the waves and spectral analysis. In this context, the model solves the wave action conservation equation employing a parametric formulation that separates directional components.

The model operates by picking out realistic point outputs for offshore wave scenarios, evenly distributed with an interval of 100 meters along the 10 meter and 15 meter contours constituting several sites in the Sydney area, including Manly beach. The data provides information on wave period, wave height and wave direction and it is possible to use the model to extract specific wave data for analysis.

A matlab code was created to extract the specific nearshore wave scenarios at Manly beach needed for testing and calibration with ShoreFor. The code starts by loading the offshore wave data retrieved from ERA5, including parameters: wave height, peak wave period, average wave direction and date information. Then it creates a structure that assigns the loaded offshore wave data for organizing and storing of the processed wave data.

Furthermore the site of interest (Manly) was specified and the depth contour was chosen to be 10 meters. Alongshore location was set to 1270 which is the value calculated from another matlab code created for the specific location of Manly beach. The final step is calling a function that loads the prepared offshore wave data, lookup-information, the depth contour and the alongshore position locations for the chosen site. A new set of variables for wave height and peak wave period representing inshore wave conditions at Manly beach was finalized. Both sets of forcing data (nearshore and offshore) was used for different purposes in following modeling scenarios.

### **5.3.2 ShoreFor GUI v1.0 setup**

All the calibrations and hindcasts in this study will be done in ShoreFor v1.0. ShoreForv1.0 is a freely available version of the ShoreFor model that comes as a GUI in MATLAB and allows users to interact with the model that was developed by Davidson, Splinter and Turner in 2013 (Davidson et al., 2013). The model requires one set of forcing data and one set of morphology observation data.

As mentioned in chapter 3.6, the model uses hindcasting as a method to predict future shoreline position by analysing earlier observed events. The model performance and reliability is tested by comparing these predictions with real events. Before hindcasting applies, the model calibrates the model parameters, which involves adjusting the model parameters or settings so that its predictions better align with real observations. This aims to reduce any errors or deviations in the model outputs, thus making the hindcast results more reliable and accurate.

### 5.3.3 Model Inputs

When running Shorefor v1.0, following parameters needs to be defined; “Shoreline measurement error (SME)” (the estimated error in the shoreline measurement data), “Water depth” (the depth at the spot where wave data is retrieved) and “d50” (sand grain size of the site). The numeric values was set to the following, depending on whether the model was trained with nearshore or offshore waves;

Table 3: Model inputs in Shorefor v1.0

Variable	Inshore location	Offshore location
SME (m)	2	2
water depth (m)	10	70
d50 (mm)	0.3	0.3

table 3 describes model inputs when running Shoreforv1.0 with local wave data (Inshore location) and wave data from era5 (Offshore location).

### 5.3.4 Initial model

Initially, the model performance was evaluated using all available shoreline data from CoastSnap and local wave data to evaluate the best case scenario. In this case calibration and hindcast rely on the same dataset. In following section, the effects on model performance was examined by degrading the shoreline data step by step with each calibration. The initial model serves as a baseline for comparing with all further calibrations, aiding in the assessment of their impact on the model’s performance.

### 5.3.5 Test cases

This section describes the methodology for examining the two key questions: 1 - "How much data is needed to train Shorefor v1.0?" and 2 - "Is inshore/local wave conditions needed in order to get good model results?".

#### 1) How much data from CoastSnap is needed to train ShoreFor v1.0?

In the first testing phase, the model performance of ShoreFor v1.0 was tested by degrading the original morphology data set by using different sets of calibration data of various sampling frequencies (days) and sampling durations (years), as can be seen in table 4 and 5.

Making the model match the observed data and testing the ability to reproduce seen data, just as was done with the initial model (chapter 5.3.4), is important but the end goal is to test how the ability of the calibrated model to accurately predict the shoreline position by using an unseen wave-time series. Therefore, the calibrations in this testing phase was presented to a "blind" hind-cast data set. This data set was created with MATLAB by extracting only the datapoints from

the last available year (Jan 1, 2022 - Dec 31, 2022). The hindcast data set, referred to as the test data from now on, will always be the same but the calibration data will be different for every model scenario. Since the hindcast data needs to be unseen to the calibration data, the calibration data timeseries always ended prior to the hindcast data. The entire data set that was used for these calibrations has data from five years. So for example, for hindcasts with various durations (see table 5), the calibration time-series ranges from one to four years and ends at the fifth year where the unseen hindcast data (test data) starts.

To examine the impact of sampling frequency, several calibrations were conducted at varying intervals from the initial data point. When determining the spacing length, guidance was drawn from the report by Kristen et. al (2013) as they used similar methods to assess ShoreFor model performance.

Table 4: Summary of calibration runs for various frequencies of shoreline sampling

Model(ID)	Frequency (Days)
F_7D	7
F_14D	14
F_30D	30
F_60D	60

table 4 presents all four subsets with various shoreline sampling frequency, all spanning from May 17, 2017 December 31, 2022. Each subset is given a unique name (Model(ID)) for easy comparison.

To assess the model performance due to calibration duration, several calibrations were executed, each spanning different durations. The decision to utilize these specific subset lengths aimed to maintain consistency and simplicity throughout the calibration process. Yearly timesteps were deemed the most suitable approach. Shorter intervals (such as monthly) were considered inadequate for credible calibrations based on previous observations (Splinter, 2013) and longer intervals was regarded as they limited the number of viable calibrations. CoastSnap supplied ~five and a half years of available shoreline data from May, 2017 to February, 2023. In order to provide yearly subset spans, all data from 2017 and 2023 was excluded from this operation.

Table 5: Summary of calibration runs for various duration lengths of shoreline sampling

Model(ID)	Duration (Years)
D_1Y	1
D_2Y	2
D_3Y	3
D_4Y	4

table 5 presents all four subsets and their duration lengths, spanning from 1:4 years with yearly timesteps starting on January 1st, 2018. Each subset is given a unique name (Model(ID)) for

easy comparison.

## **2) Is inshore/local wave conditions needed in order to get good model results when training the ShoreFor model with CoastSnap data?**

In this part of the testing phase, the model performance when training the model with the original offshore wave data from ERA5 will be compared to the initial model that was run with the transformed nearshore data.

### **5.3.6 Test result analysis**

The ShoreFor model's executed hindcast results offer the following parameters for analysis; Root Mean Square Error, Normalized Mean Square Error, Correlation Coefficient, and Brier Skill Score.

#### **Root Mean Square Error (RMS-error)**

The RMS-error calculates the average square root of individual error values. It provides quantitative indication on the difference between the model's predicted values and the actual observed data values. Lower RMS error indicates better alignment between model predictions and observations.

#### **Normalized Mean Square Error (NMS-error)**

The NMS-error is a variation of the RMS-error where RMS values are normalized using the mean of the actual data values. This normalization is done to relate error values to the actual values and provide a proportional perception of accuracy in relation to the scale of data values. Normalization can be useful when comparing errors between different datasets that may have different magnitudes.

#### **Correlation coefficient (r)**

The correlation coefficient assesses the relationship between the model's predicted values and the actual values. Higher positive r indicates strong agreement.

#### **Brier Skill Score (BSS)**

BSS is commonly used in weather forecasts and assesses the model performance in comparison to a reference model by comparing model residuals to a baseline. It includes both accuracy and reliability in the forecasts. It ranges from  $-\infty$  to 1, where 1 indicates a perfect model and 0 indicates a poor model. Negative values suggest that the model is worse than a simple constant model. In general, the reliability of the values ranges from:  $< 0.3$  "fair"  $< 0.6$  < "good"  $< 0.8$  < "excellent" (Davidson et al. 2013).

#### **Akaike Information Criterion (AIC)**

AIC is used for measuring model performance in statistics and machine learning. It balances the model's fit to the data with its complexity by penalizing overfitting and is calculated based on the log-likelihood and number of parameters. Lower AIC indicates better fit between the data and the model.

#### **PERCENT TIME CORRECT (PTC)**

PTC is a measure of performance or accuracy for a given task or model in data science, used to evaluate how well a model or system operates over a period of time. It measures the percentage of

time where a model or system correctly identifies or predicts the outcome or behavior of a given event or observation. The higher the percentage, the better the model or system performs.

## 6 Results

### 6.1 Part 1: Impacts of La Niña

The result for part 1 is presented in the following section. Firstly the change in beach width is presented for each beach along with the wave height for the same period. The annual beach width change and the end point change is also presented in each graph. For each beach and graph a non-linear regression analysis is also shown. A figure showing the distribution of the data for all beaches as well as a table showing the amount of data available and used in the study for the different sites is also presented.

#### 6.1.1 Alexandraandra Headland Beach

In figure 24 the change in beach with as well as the wave height for the same time period is presented. The time series reaches from the end of 2021 until the beginning of 2023. A decrease in beach with can be seen.

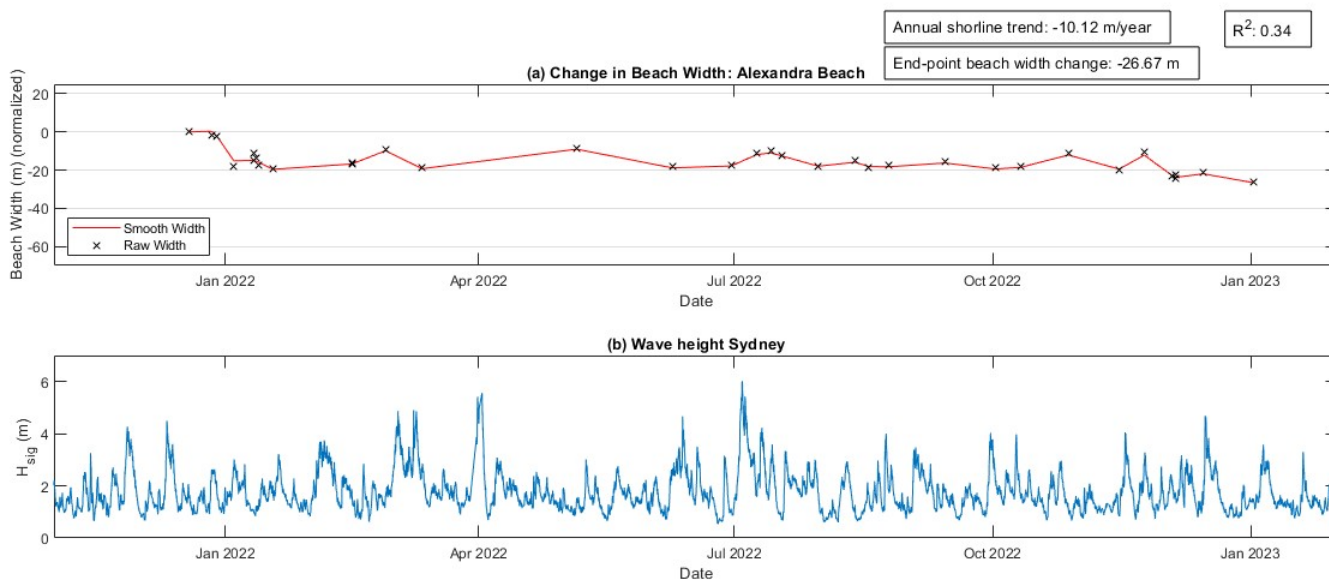


Figure 24: a) Change in beach with of Alexandraandra headland beach. b)Wave height data Sydney.

In figure 25 a linear fit can be seen between the wave height and the beach width. In this graph an analysis can be made in how well high waves correlates with a decrease in beach width for this particular beach.

The x-axis represents the interpolated wave height, and the y-axis represents the normalized beach width. Each scatter point on the plot represents a pair of corresponding measurements of wave height and beach width. The linear fit line indicates the best linear approximation of the relationship between these two variables. If the line has a negative slope, it suggests that higher wave

heights are associated with decreased beach widths, which might be indicative of erosion processes.

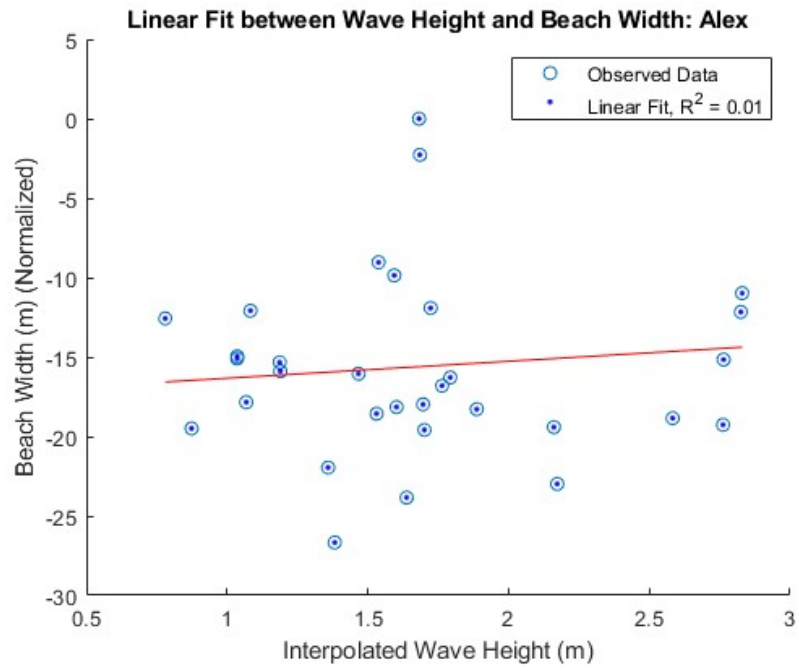


Figure 25: Linear regression analysis for Alexandra Headland Beach.

### 6.1.2 Buddina Beach

In figure 26 the change in beach width as well as the wave height for the same time period is presented. The time series reaches from the end of 2021 until the end of 2022. A slight decrease in beach width can be seen.

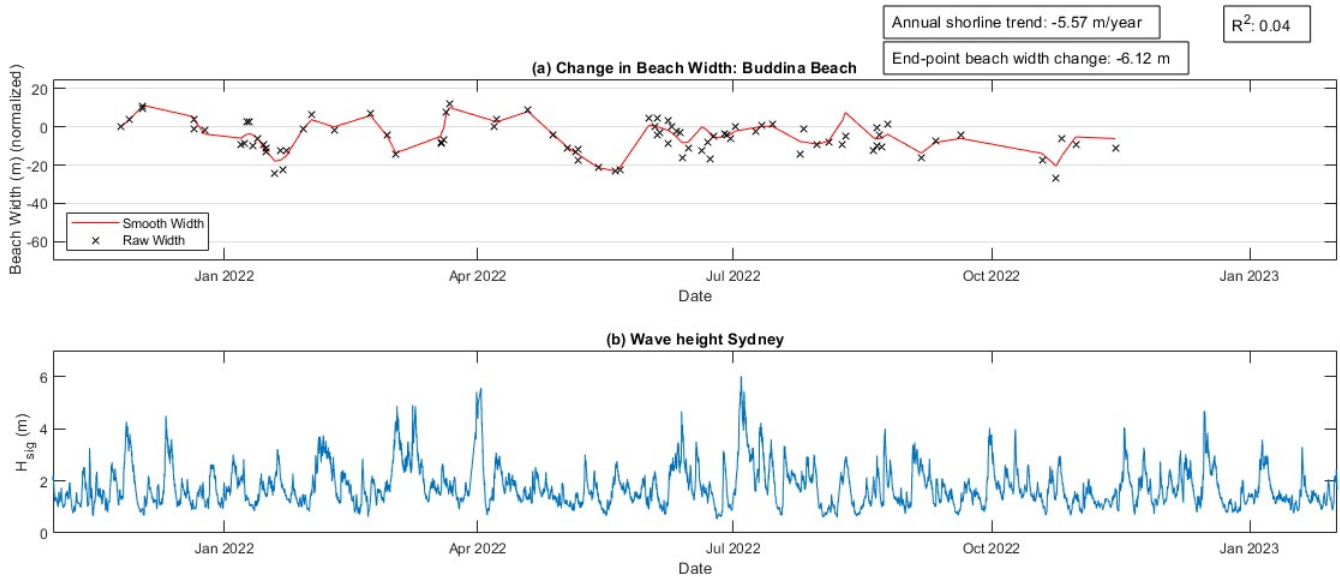


Figure 26: a) Change in beach width of Buddina beach. b) Wave height data Sydney.

In figure 27 a linear fit can be seen between the wave height and the beach width. In this graph an analysis can be made in how well high waves correlates with a decrease in beach width for this particular beach.

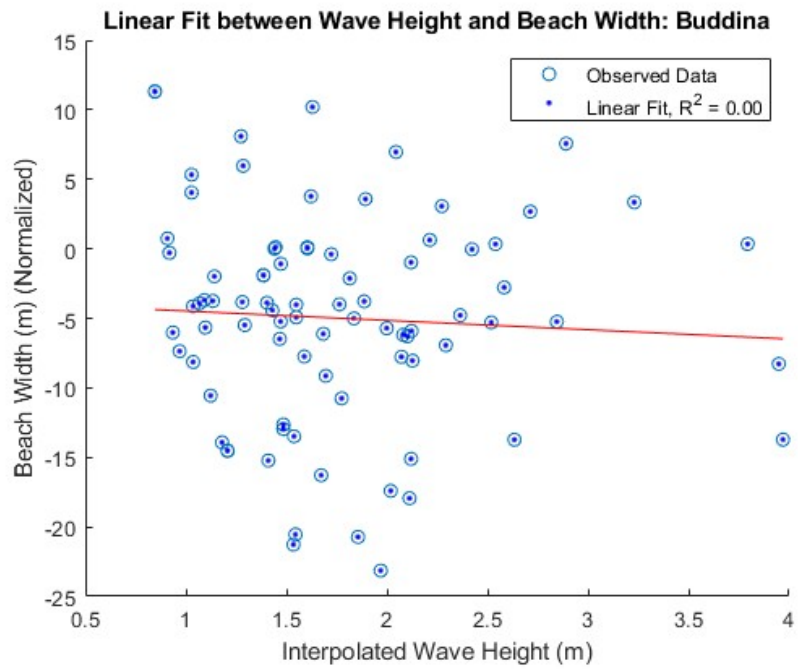


Figure 27: Linear regression analysis for Buddina Beach.

### 6.1.3 Stockton Beach

In figure 28 the change in beach with as well as the wave height for the same time period is presented. The time series reaches from the beginning of 2020 until the beginning of 2023.

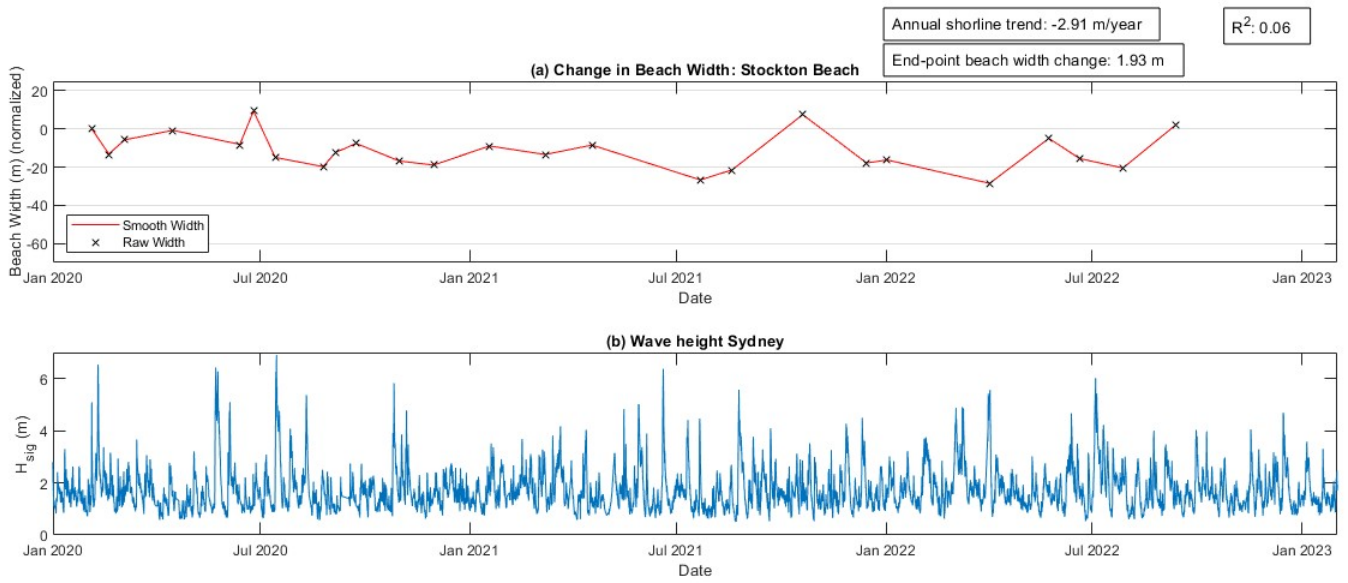


Figure 28: a) Change in beach width of Stockton beach. b) Wave height data Sydney.

In figure 29 Linear fit can be seen between the wave height and the beach width. In this graph an analysis can be made in how well high waves correlates with a decrease in beach width for this particular beach.

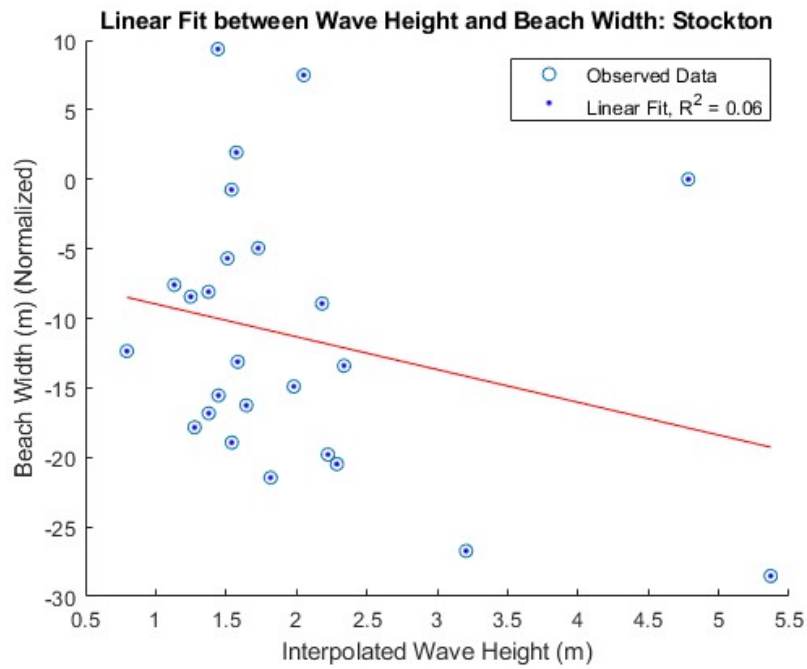


Figure 29: Linear regression analysis for Stockton Beach.

### 6.1.4 Blacksmiths Beach

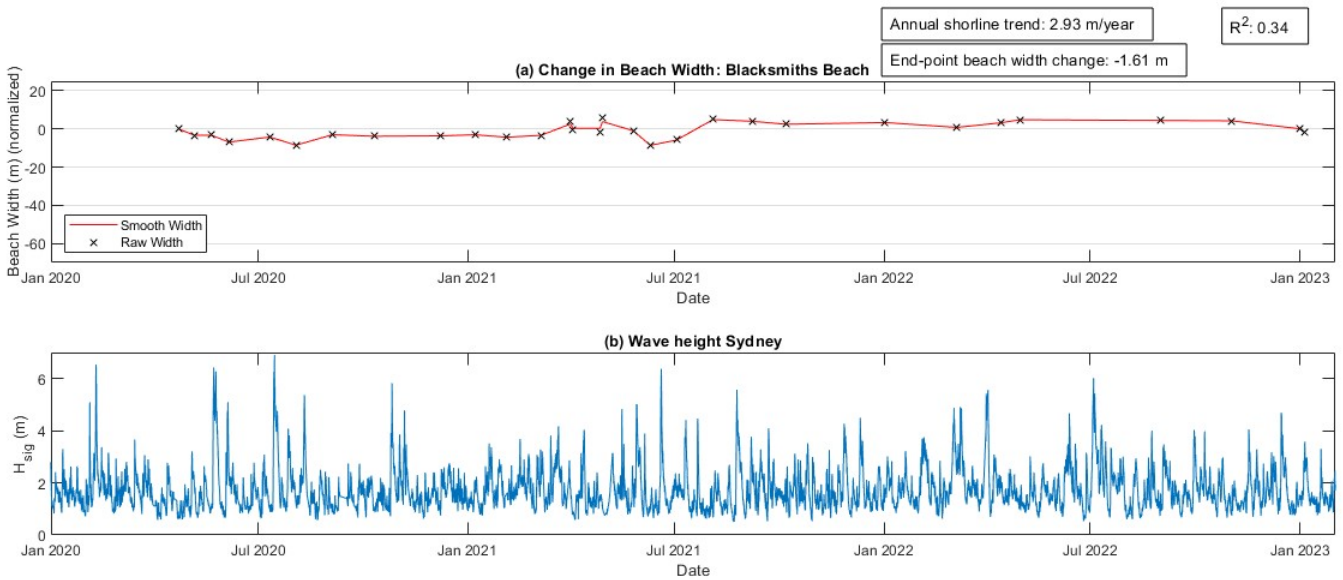


Figure 30: a) Change in beach width of Blacksmiths beach. b) Wave height data Sydney.

In figure 30 the change in beach with as well as the wave height for the same time period is presented. The time series reaches from the beginning of 2020 until the beginning of 2023.

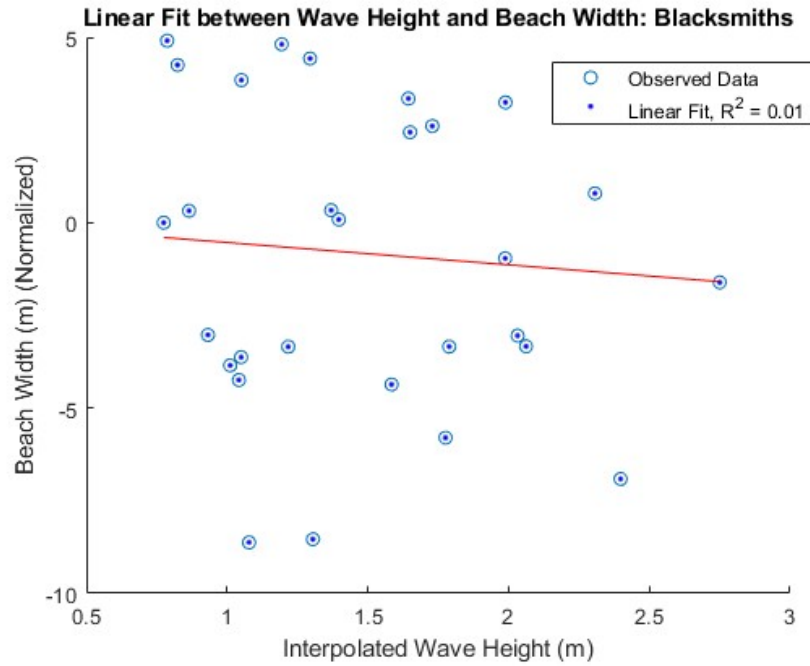


Figure 31: Linear regression analysis for Blacksmiths Beach.

In figure 31 a non-linear fit can be seen between the wave height and the beach width. In this graph an analysis can be made in how well high waves correlates with a decrease in beach width for this particular beach.

### 6.1.5 North Narrabeen Beach

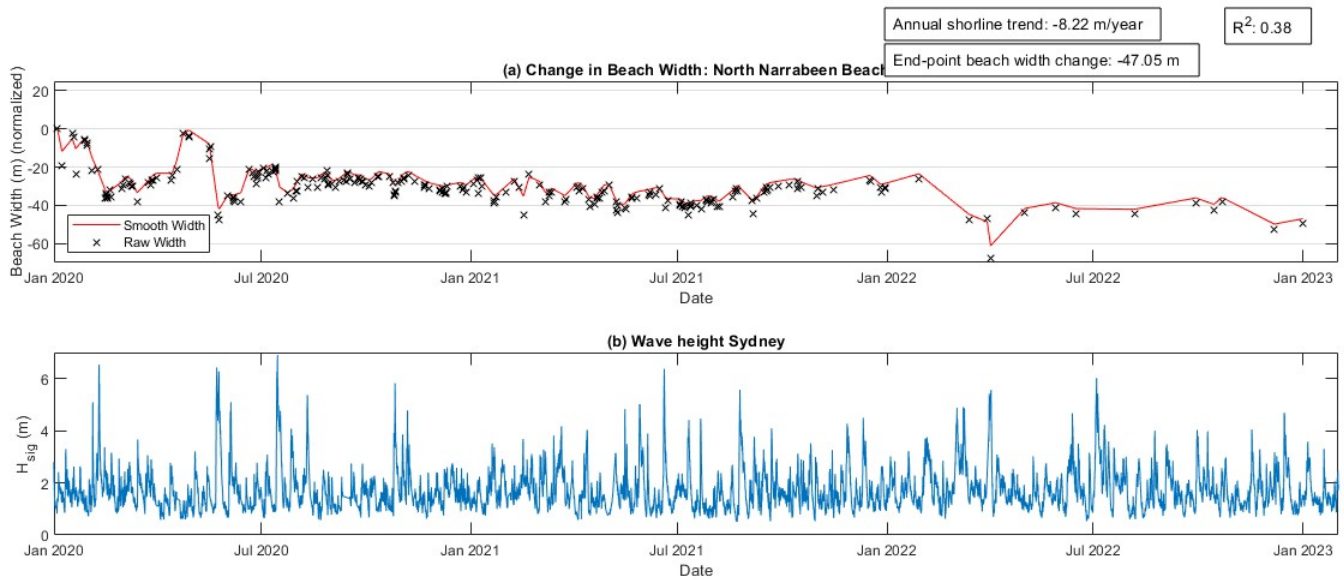


Figure 32: a) Change in beach width of North Narrabeen beach. b) Wave height data Sydney.

In figure 32 the change in beach width as well as the wave height for the same time period is presented. The time series reaches from the beginning of 2020 until the beginning of 2023. A decrease in beach width can be seen.

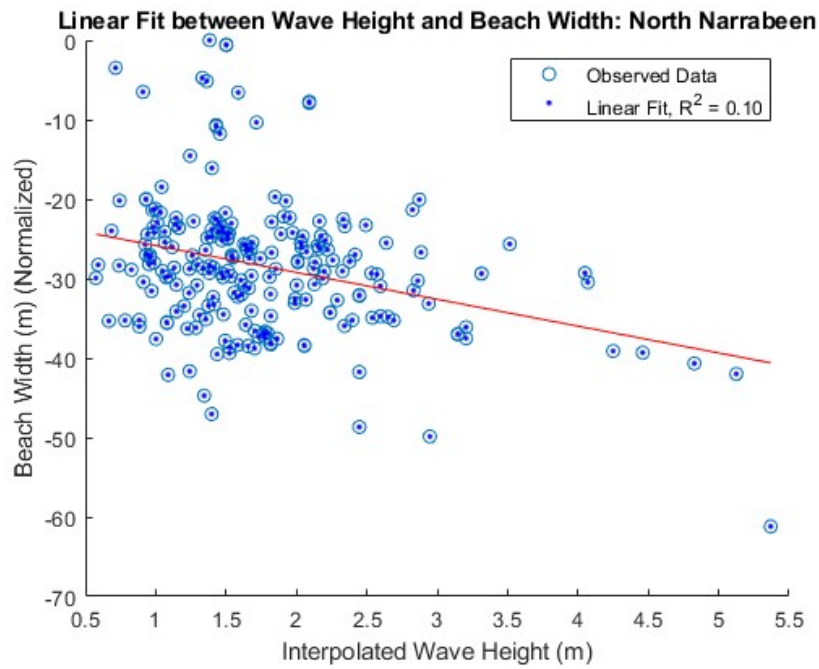


Figure 33: Linear regression analysis for North Narrabeen Beach.

In figure 33 a linear fit can be seen between the wave height and the beach width. In this graph an analysis can be made in how well high waves correlates with a decrease in beach width for this particular beach.

## 6.1.6 Manly Beach

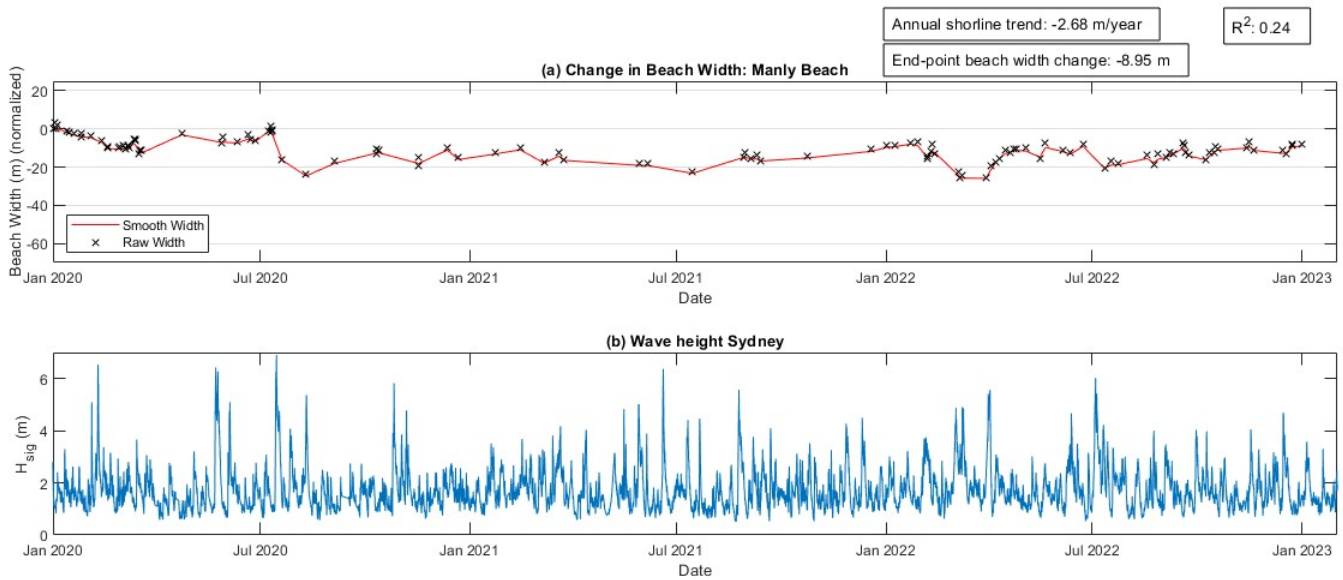


Figure 34: a) Change in beach width of Manly beach. b) Wave height data Sydney.

In figure 34 the change in beach width as well as the wave height for the same time period is presented. The time series reaches from the beginning of 2020 until the beginning of 2023. A decrease in beach width can be seen.

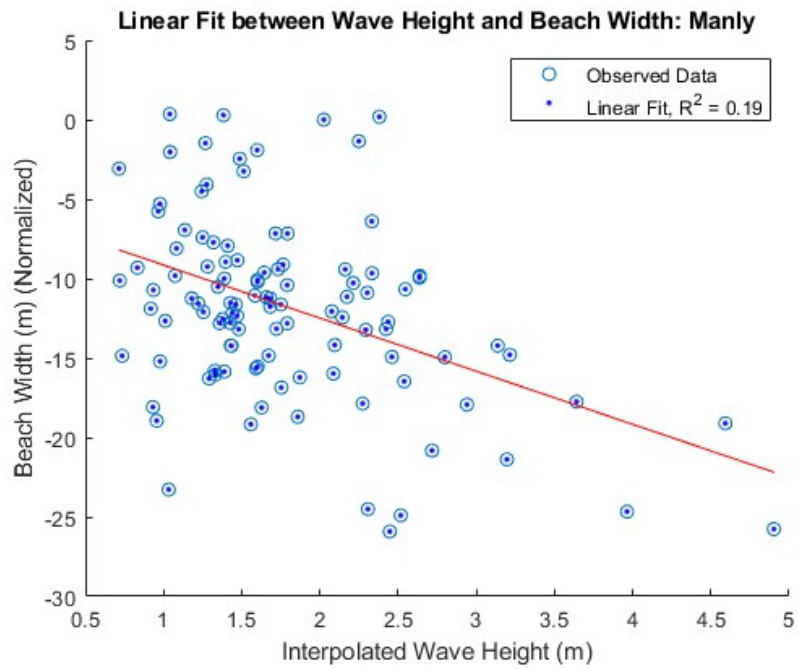


Figure 35: Linear regression analysis for Manly Beach.

In figure 35 a linear fit can be seen between the wave height and the beach width. In this graph an analysis can be made in how well high waves correlates with a decrease in beach width for this particular beach.

### 6.1.7 Broulee Beach

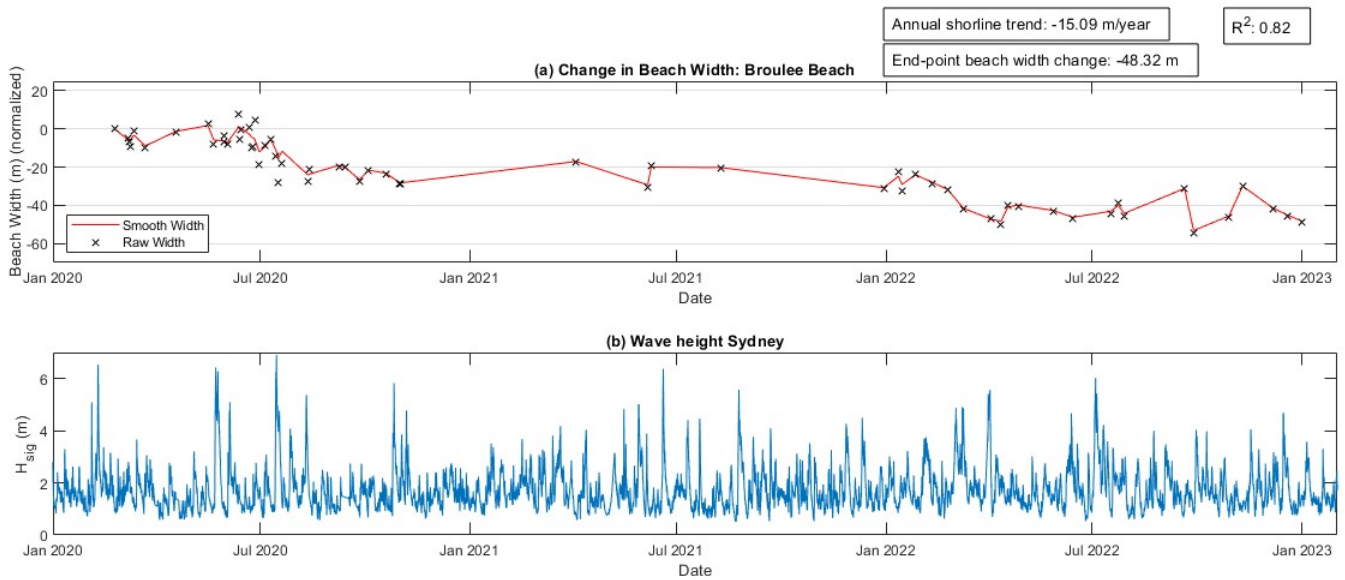


Figure 36: a) Change in beach width of Broulee beach. b) Wave height data Sydney.

In figure 36 the change in beach width as well as the wave height for the same time period is presented. The time series reaches from the beginning of 2020 until the beginning of 2023. A decrease in beach width can be seen.

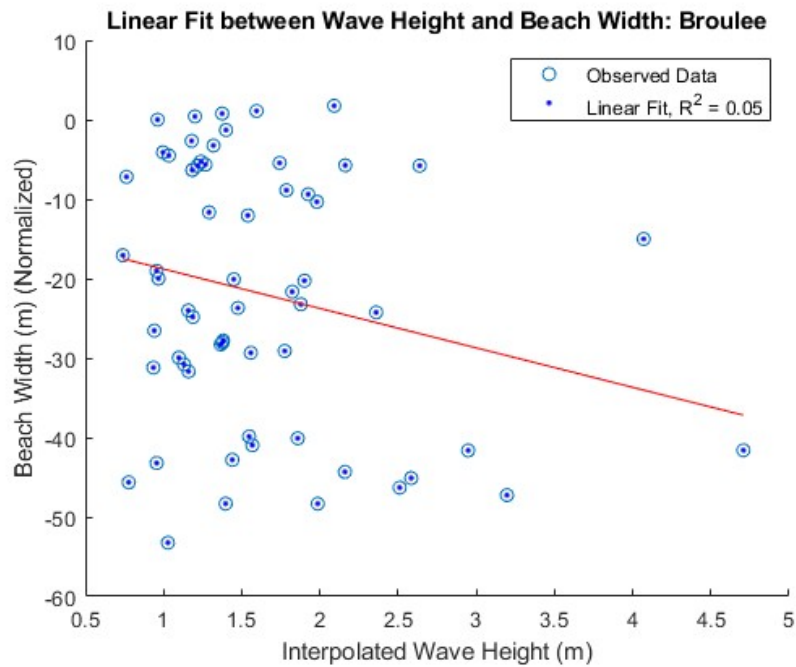


Figure 37: Linear regression analysis for Broulee Beach.

In figure 37 linear fit can be seen between the wave height and the beach width. In this graph an analysis can be made in how well high waves correlates with a decrease in beach width for this particular beach.

### 6.1.8 Combined results

Table 6: Shoreline change

Beaches	Annual shoreline change (m/year)	R <sup>2</sup>	End-point beach with change (m)
Alexandra Headland Beach	-10.12	0.34	-26.67
Buddina Beach	-5.57	0.04	-6.12
Stockton Beach	-2.91	0.06	1.93
Blacksmiths Beach	2.93	0.34	-1.81
North Narrabeen Beach	-8.22	0.38	-47.05
Manly Beach	-2.68	0.24	-8.95
Broulee Beach	-15.09	0.82	-48.32

In figure 38 the combined results for both the annual trend and the end-point results can be shown. Here all the locations results are presented in a bar chart. The Average over all the locations for both the annual and end-point is also shown in this figure.

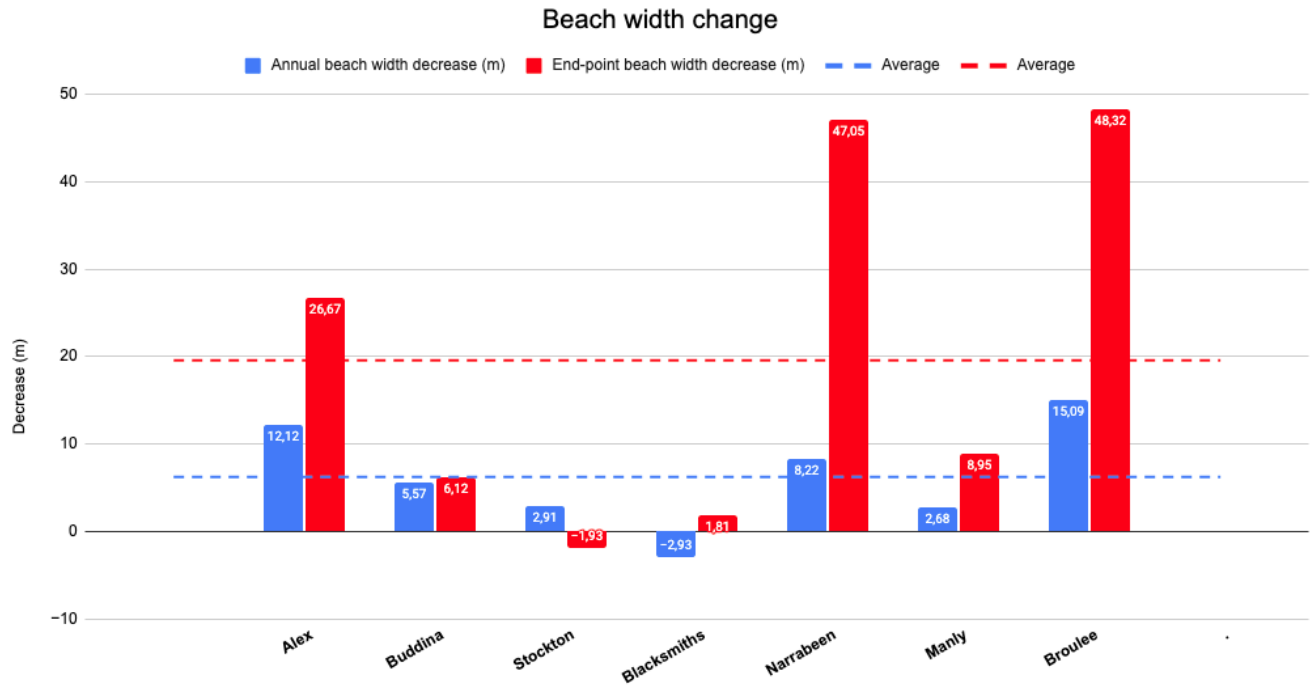


Figure 38: Combined results of beach width change.

### 6.1.9 Data distribution

In table () the distribution of the data is shown. In the first column the name of the beach as well as the duration of time (days) that data was available. In other words for how long of a period images had been submitted to that particular Coastsnap site. The second column shows the total amount of images available for that time period. The third column shows the amount of images used in the time series. The selection process is explained in the methodology part of this report. The fourth column is the

Table 7: Images

Beaches (period with existing data)	Total Images	Used Images	Images/month
Alexandra Headland Beach (380)	58	34	2.7
Buddina Beach (355)	210	86	7.7
Stockton Beach (952)	36	25	0.8
Blacksmiths Beach (989)	45	30	0.9
North Narrabeen Beach (1094)	513	251	6.9
Manly Beach (1097)	413	116	3.2
Broulee Beach (1043)	138	61	1.8

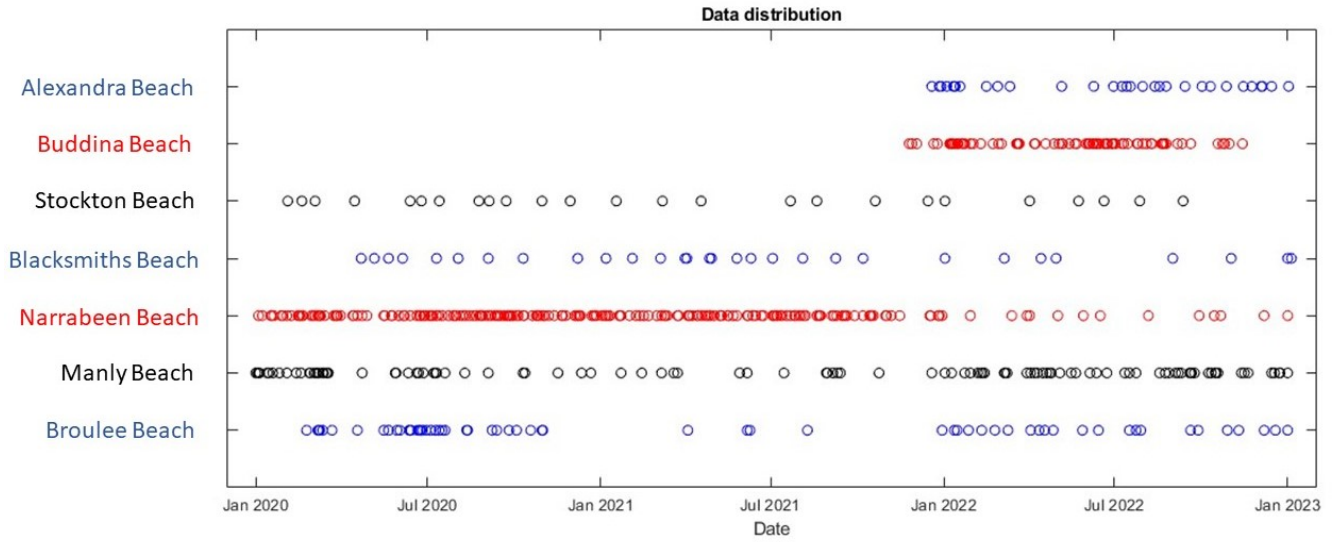


Figure 39: Data distribution.

## 6.2 Part 2: Shoreline modeling

The first section of the results from Shoreline modeling with CoastSnap data presents the model performance when it is shown all the available observations from Manly beach and transformed local wave conditions.

### 6.2.1 Initial model

Table 8: Initial model run with all available local data

Model (ID)	Hindcast results					
	RMSE (m)	NMSE (m)	r	BSS	AIC	PTC (%)
Initial_model	5.2527	0.52986	0.68567	0.62023	3671.6892	77.0115

Table 8 presents all hindcast results from running the model with all available morphology observations from CoastSnap and forcing data at inshore wave location. ~77% of the time the model was within the uncertainty of the shoreline measurements ( $\pm dx$ ), and had an overall correlation of ~0.69 and a NMSE of ~0.50. Compared to the baseline model (a linear trend), the shoreform model showed significant improvement with a Brier Skill Score of ~0.62.

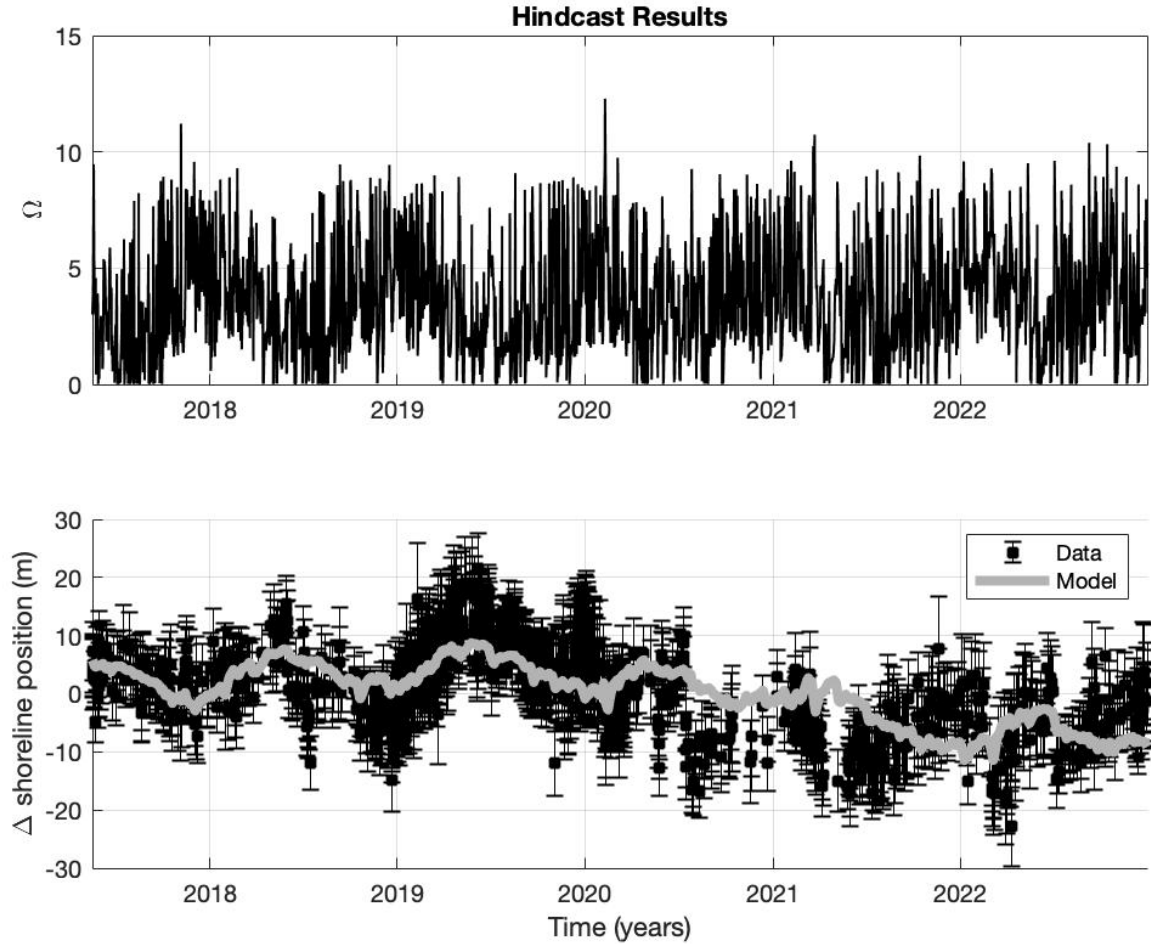


Figure 40: Initial model hindcast results

Figure 41: Graphics of variations in optimized  $\Omega$  eq timeseries (top) and change in shoreline position over time (bottom) for the Initial model. The black squares in the bottom graph represent the actual observed values of the shoreline, with error bars around them indicating the uncertainty in the measurements. The gray line represents the model's prediction of the shoreline. Here, around the end of the year 2020 as well as the beginning of 2021, one can see that the model's predictions deviate slightly as chunks of data is missing. This can be linked to the Dean number  $\Omega$ , that deviates at the same points.

### 6.2.2 Test cases

Following section will present the impact of degrading data (both in calibration length and sampling) and in using inshore (local) vs offshore (era5) wave data.

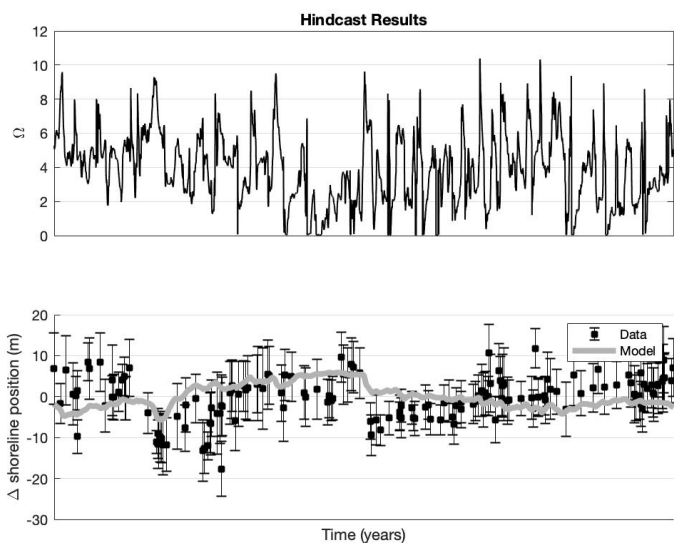
#### 1 - "How much data is needed to train ShoreFor v1.0?"

Table 9 presents all hindcast results from running the model with various data sampling frequen-

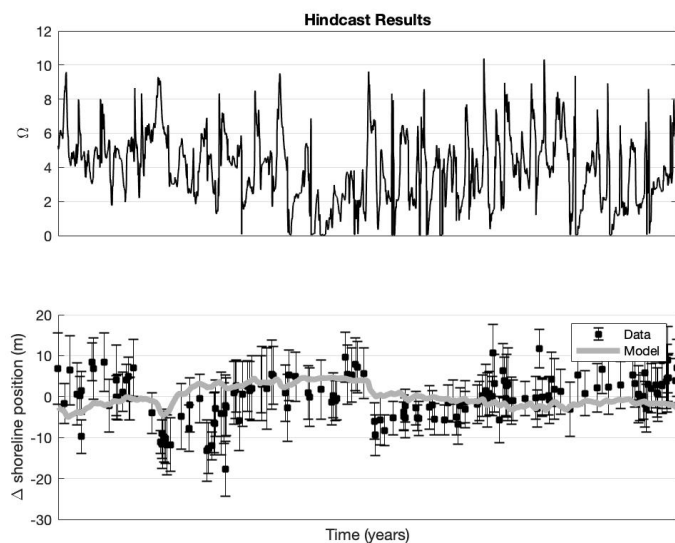
Table 9: Summary of model runs with various frequencies of shoreline data sampling

Model (ID)	Hindcast results					
	RMSE (m)	NMSE (m)	r	BSS	AIC	PTC (%)
F_7D	5.7673	1.1881	0.090495	0.55547	519.7343	66.8831
F_14D	5.788	1.1966	0.10226	0.54963	520.2145	67.5325
F_30D	5.7614	1.1857	0.034871	0.56297	519.5991	69.4805
F_60D	5.7585	1.1845	0.13123	0.56242	519.5303	68.1818

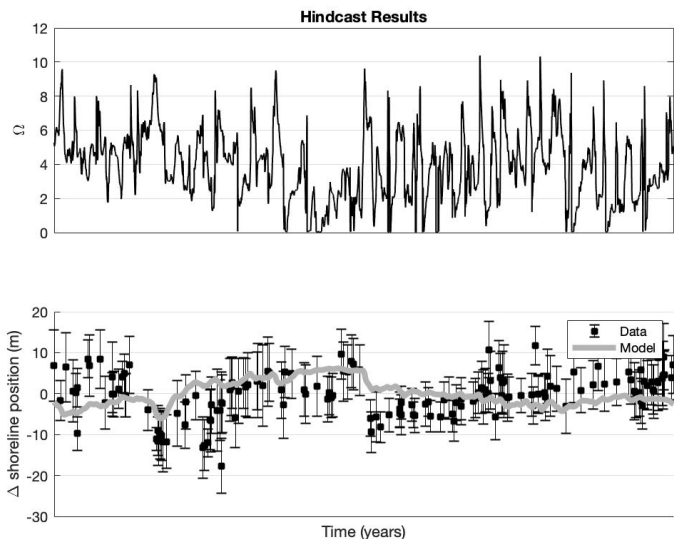
cies of shoreline data. NMSE and AIC values appear nearly unchanged regardless of sampling frequency. However, wider spacing tends to generate higher PTC and r-values. All BSS-values are  $< 0.6$  and  $> 0.3$ , however, higher data sampling frequency shows BSS-values are slightly increasing.



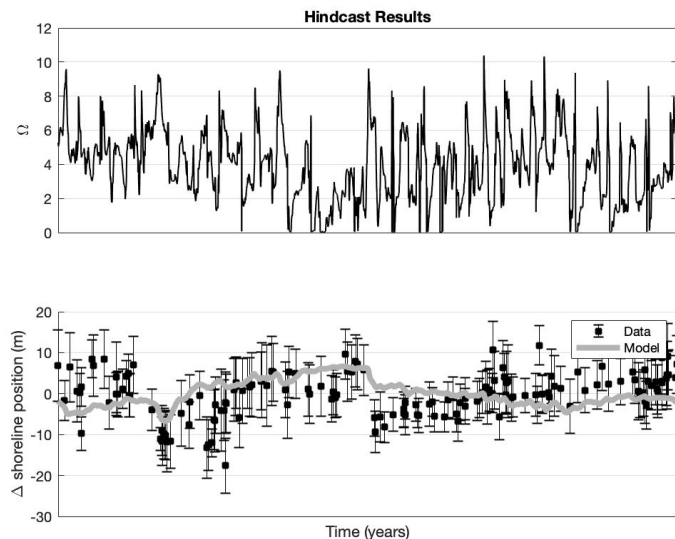
(a) F\_7D hindcast results



(c) F\_30D hindcast results



(b) F\_14D hindcast results



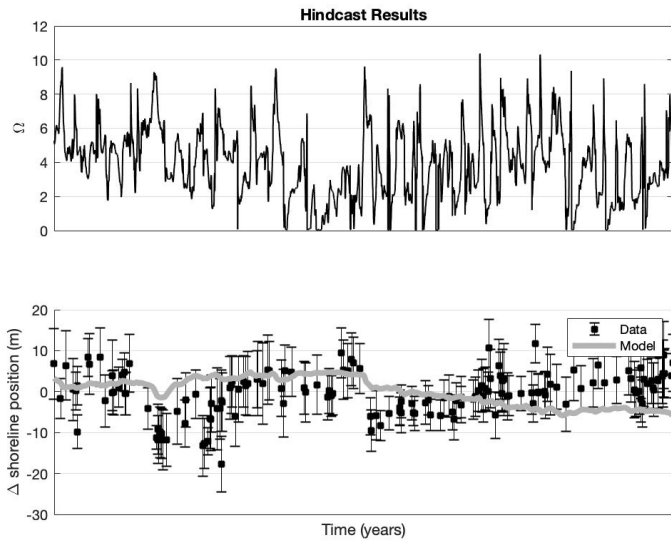
(d) F\_60D hindcast results

Figure 42: Optimized  $\Omega$  eq timeseries (top) and change in shoreline position over time (bottom) for shoreline sampling frequency = 7 days (a), = 14 days (b), = 30 days (c) and = 60 days (d). The time span for each calibration only includes the test data, which contains all the data from 2022.

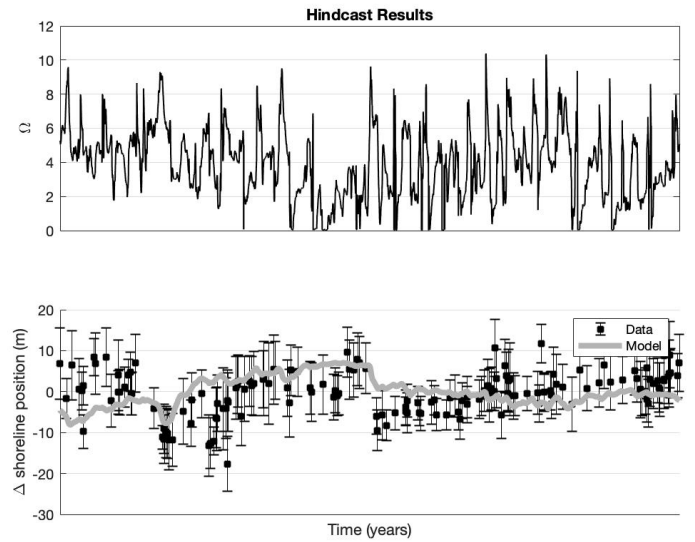
Table 10: Summary of model runs with various duration lengths of shoreline data sampling

Model (ID)	Hindcast results					
	RMSE (m)	NMSE (m)	r	BSS	AIC	PTC (%)
D_1Y	6.6568	1.5828	-0.13652	0.66303	538.9214	61.039
D_2Y	5.9472	1.2633	0.13676	0.44204	523.8429	70.7792
D_3Y	6.0253	1.2968	0.092986	0.5412	525.5891	66.8831
D_4Y	5.6094	1.1239	0.10868	0.58937	516.021	68.8312

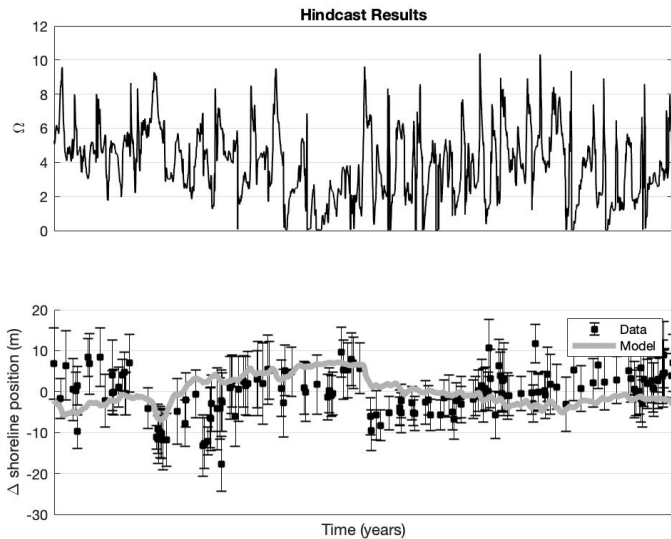
The hindcast results from running the ShoreFor model with various sets of yearly durations is presented in table 10. The outcome demonstrates varied performance across different time periods (1 to 4 years) for the models. Generally, longer data sampling durations show lower NMSE and higher PTC. The correlation coefficient decreases with duration length marginally, while test run D\_1Y stand out with a negative value. All models runs have BSS values  $> 0.3$ , but only D\_1Y and D\_4Y generates values  $\geq 0.6$ .



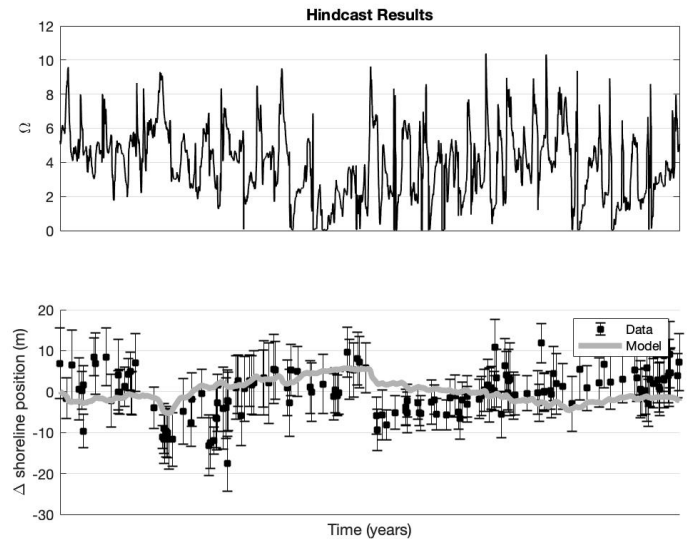
(a) D\_1Y hindcast results



(c) D\_2Y hindcast results



(b) D\_3Y hindcast results



(d) D\_4Y hindcast results

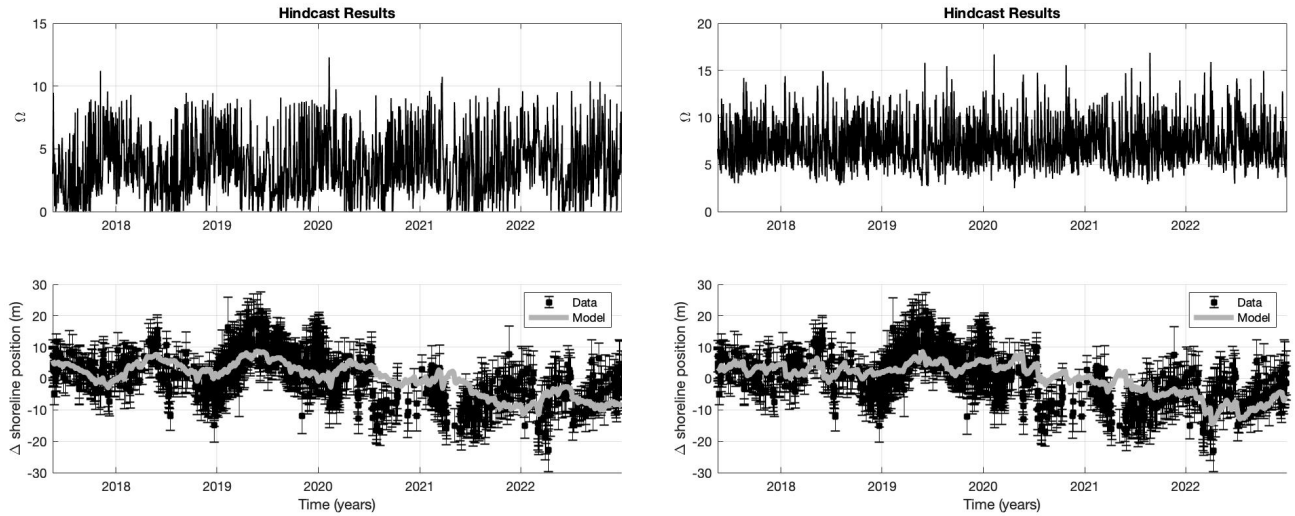
Figure 43: Optimized  $\Omega$  eq timeseries (top) and change in shoreline position over time (bottom) for shoreline sampling duration = 1 year (a), = 2 years (b), = 3 years (c) and = 4 years (d). The time span for each calibration only includes the test data, which contains all the data from 2022.

## 2 - "Is inshore/local wave conditions needed in order to get good model results?"

table 11 presents all hindcast results from running the model with all available morphology observations from CoastSnap, once with inshore wave conditions and once with offshore wave conditions. Metrics show that the Initial model has demonstrated slightly lower NMSE, slightly higher correlation coefficient and BSS is  $> 0.6$  for both models.

Table 11: Model runs with all available shoreline data from Manly beach and nearshore (Initial model) vs offshore wave data

Model (ID)	Hindcast results					
	RMSE (m)	NMSE (m)	r	BSS	AIC	PTC (%)
Initial model	5.2527	0.52986	0.68567	0.62023	3671.6892	77.0115
Offshore model	5.3292	0.54541	0.67428	0.63528	3685.8931	72.9443



(a) Nearshore accuracy results

(b) Offshore accuracy results

Figure 44: Optimized  $\omega$  timeseries (top) and change in shoreline position over time (bottom) for Initial model (a) and Offshore model (b). Compared to the Initial model, it shows that the model predictions (gray line) correlates more irregularly with the observed values.

## 7 Discussion

### 7.1 Part 1: Impacts of La Niña

#### 7.1.1 Time-series

In figure 38 and table 7 the beach width change for all the study sites can be seen. The first thing to be noted is that all the sites except Blacksmiths beach show a negative trend in beach width change, meaning decrease over time. The same is true for the end-point beach width change, with the only site showing a positive result in Stockton beach. The average over all sites for the end point change is just under 20 m and the average for the annual trend is around 6 m/year. What is interesting to note for both Blacksmiths and Stockton is that, Blacksmiths show a positive trend over time but show a slight negative change for the end-point change, while Stockton shows a positive end point change but a slight negative trend over time. None of the values for either Blacksmiths or Stockton are deviating far from 0, and with their conflicting results it can be concluded that none of these two beaches show any significant change in either shoreline recession or accretion.

Besides Blacksmiths and Stockton all the other sites have from the results clearly experienced

shoreline recession. Buddina beach and Manly beach both show a slightly lower change and trend than the other remaining three, but have still very clearly eroded. Alexandra shows a high negative change for the shoreline end-point value. To be noted and remembered is that Alexandra headland beach only have data for about a year making the value -26.67 m a very large negative value. North Narrabeen beach shows a value for the end-point result of -47.05, and a annual shoreline change trend of -8.22. In figure 32 it can be seen that there seems to be some events in the beginning of the time series that have contributed to more severe erosion, but after that quite a steady decline in beach width is shown. There are clear dips can be seen in figure 32. The first during around March 2020 - May 2020. The second one around June 2020, And later around April 2022, which also is the lowest value for the whole time series.

Broulee beach shows the most change over the three year time period with a shoreline end-point change of 48.32 m. The annual trend is also the highest for all the sites with a annual trend of -15.09 m/year. In figure 36 it can be seen that Broulee shows a relatively steady decline in beach width, with no clear events of recovery. One thing to be noted is that around April 2022 a dip can be seen for Broulee as well. Looking further into this, also manly show this in figure 34, and Stockton as well in figure 28. To know what is related to this dip, meteorological data would have to be investigated. Alternatively looking more closely at the images around this point to see any signs of a storm event. What can be seen from the wave data is that there is a peak in wave height during these dips.

Something to be noted is that the magnitude of the erosion for the different beaches vary a lot. The magnitude of the end-point results can of course not be compared directly for all the beaches since the timeline is not the same. But both Blacksmiths and Stockton cover about the same time as Narrabeen beach and Broulee, and the results differ a lot. For Blacksmiths and Stockton the end-point results are either positive and very close to zero. While for Narrabeen and Broulee the end-point value is 47,05 m and 48,37 m. According to the findings in the article by Melissa A. Bracs et al. (2016) a conclusion was made that the two locations showed regionally coherent behavior in response to common environmental forcing. In this study the sites were located 35 km apart. The beaches Blacksmiths beach and North Narrabeen beach is located about 130 km apart. Both Blacksmiths beach and North Narrabeen beach are both located in the Southern NSW region, but since these show such different results they might be too far apart to show the same effects as shown in the study by Melissa A. Bracs et al. (2016). In figure 14 compared to figure 14 it can be seen that North Narrabeen has a slight more southern direction than Blacksmiths beach which could according to the background result in lower waves, since the energy of the waves originates for the most part from the southern swell. What can be noted from the satellite image from Blacksmiths 12 is that a breakwall is located on in the south end of the beach where the coast snap station is located. As mentioned in the background, breakwalls act as a barrier for the waves and is a well used management technique for coastal erosion. For Stockton a kind of breakwall is also present in the south end of the beach close to the CoastSnap station. These breakwalls located at both Blacksmiths and Stockton, could in combination with the results seen that they indicate very little to no erosion compared to the other study sites, indicate that the breakwalls are effective in minimising beach erosion and recession.

Another interesting result is Alexandra beach and Buddina beach. They both cover about a year and is located very close geographically. The only thing separating the beaches is a headland. How come the result for the annual trend is about the double decrease for Alexandra than for

Buddina and the end-point about four times the decrease for Alexandraandra compared to Buddina? It is hard from just these results to draw a definite conclusion, but since the only obvious difference is the slight difference in direction of the two beaches and the headland that separates them. One reason could be difference in longshore transport. From the theory it is known that the headland should obstruct the longshore transport somewhat, and on this part of the coast the general direction of the longshore transport should be towards the north. And in figure 11 where the camera location is demonstrated it can be seen that the coast snap station is located exactly where the longshore transport should be obstructed and slowed. Since the two beaches are located so close geographically this might be the reason for the difference in erosion observed. This also since according to the research by Melissa A. Bracs et al. (2016) regionally closely located beaches should behave similar to similar in response to common environmental forcing.

To be noted also is that Manly Beach and North Narrabeen beach shows quite different magnitudes of erosion even though they are located very close, about 10 km. Again according to Melissa A. Bracs et al. (2016) they should behave similar in response to common environmental forcing. It is therefore interesting to note what could be the reason behind the difference in results. In figure 18 the locations of both Manly Beach and North Narrabeen beach can be seen as well as the location of the coast snap stations. In figure 17 a more clear image of Manly beach and its surroundings is shown. From this it can be noted that the southern part of Manly beach where the CoastSnap station is located is much more protected from the open sea than the North part of Narrabeen beach where the CoastSnap station for Narrabeen is located. Since we know that the magnitude of the waves have a big impact on erosion and sand transport this could be the reason for the difference in the results.

In figure 5 as mentioned earlier the La Niña period can be seen to start in March/April 2020. What's interesting to see is that those time series that reaches so far back (Narrabeen, Manly, Broulee) a quite clear drop in beach width can be seen from the start of 2020 to the second part of the year. These locations that show the clearest change over all also show the clearest patterns that relates to the theory. These three beaches seem very responsive? These three beaches also have a dip in around March/April 2022. In figure 2 it can be seen that the sea surface temperatures was on normal levels during July 2021 but then lowered again. Later in March 2020 when the sea temperatures are significantly low again a drop in the beach width happens for all these three beaches. From the theory it said that more perspiration could be expected during La Niña years. Especially during spring and winter but also during the years other months. It also said that the greater the sea temperature difference from normal conditions the the larger the response in precipitation will be. From the theory it also was stated that higher precipitation is linked to more erosion. So from this, the greater the sea temperature difference from normal conditions the greater the response in erosion. Especially since it is also known from the theory that La Niña also increases the severity and frequency of storms. And that higher precipitation can cause flooding which also contributes to beach erosion. From this it seems that Narrabeen, Manly and Broulee all show results confirming the theory.

From the theory we know that wave height contributes greatly to the magnitude of shoreline recession occurring. It is therefore interesting to analyze the linear regression presented for each beach. If a connection can be made between wave height and beach width from the data-sets it supports the claim that Coast Snap data can be used for research on coastline change. For the results to be aligned with the theory what wants to be seen is a connection that shows lower beach

width connected to higher wave heights. A great example is figure 33 where we can see the linear regression for North Narrabeen beach. It can clearly be seen that a lower beach width is connected to a higher wave height. Similar can be seen in several of the Beaches. The most clear connection is shown in the location where the general erosion over all was larger. A connection can also be seen with just visually analyzing the timeseries, as mentioned in previous paragraphs.

One last thing to be noted that only images and wave data are available in this study to draw conclusions on what could have caused the erosion. From the background we know that sand transport and beach erosion is a complicated matter and many factors are playing a part in the sand transport a location is experiencing. We know for example that how the rips behave locally can play a big role.

### 7.1.2 Data distribution

In table 7 and figure 39 the amount of data available and the distribution of it is represented. In table 7 both the total amount of data available and the images used for the finished timelines, figure 24 - 36, is compiled. In relation to the time periods the average amount of images per month are listed for all sites. From figure 39 the data distribution of the data used in the timelines are shown.

In section 3.5.1 in a study by Yanxia Liu et al. (2013) satellite images were used to detect shoreline change. 32 images over 36 years were used, which results in 0.89 images per year. In the study by Antoine Deburghgraeve et al. (2023) CoastSnap images were also used, here 65 images over 9 months, resulting in 7.2 images/month. For the study by Carmen E. Elrick-Barr et al. (2023) approximately 2 images per month were used over a period of 7 months. This can be compared to the results in table 7 to get an idea if the amount of data used from the 7 study sites were enough to conduct research. The lowest quantity of data is for Stockton Beach with 0.8 images/month, closely followed by Blacksmiths Beach with 0.9 images/month. In figure 39 it can be seen that Blacksmiths has data for around one image per month but two bigger gaps in the data can be detected during 2022. The other study sites have over 1 image per/month with relatively even distributed data. One thing to note is that Broulee Beach is well documented but has two bigger gaps in the data. Here no images at all were available. According to Dr. Mitchell Harley which supervised this project and has founded the project CoastSnap, there was issues with the sign at the site. Apparently it went missing. The gaps detected for the data highlights one of the issues with citizen collected data. It is hard to control how many and when data is collected. The problem that can arise is that not enough data is available for any conclusions or that data is missing for interesting periods, for example big events of erosion. One thing to note that the sites (Stockton and Blacksmiths) that had the lowest rate of images/month also showed the least impact of erosion. With a higher quantity of data the end-point results would be the same, but the annual trend could be different. In theory the data points could have accidentally captured days when the beach had recovered and missed days after erosion events. Since the end point results for both sites were close to 0, this probably is not the case, but it can't be ruled out. This is why more data is possible is always better. The higher quantity of data available the more variability on a shorter time-frame can be seen. For example seeing the effects of specific erosion events.

In the case of this study however the data seems to be enough. In the study by Smith, R. K. and Benson, A. P (2001) he states that data should be collected with a monthly interval to "enable a representative sample of natural beach change to be measured". This is the case for 5 study sites and for the remaining to the quantity is just slightly under 1 image/month. The data for the 7 study

sites is also shown to be relatively evenly distributed. This together with the fact that the results are in line with what is expected in terms of shoreline recession during La Nina, conclusions can be taken that the data available from CoastSnap is enough to draw the conclusion that the results are reliable. And from this point to the conclusion that CoastSnap data is a good alternative for data when conducting research on coastal erosion.

From this study the results in erosion for the 7 study sites can be seen during the last La Nina event. But to be noted is that Smith, R. K. and Benson, A. P (2001) points out in their research that if the potential long term effects of ENSO is of interest, data samples needs to be present for both the La Niña and El Nino period, which is not available in this report. This means that even though conclusions can be made about the effects of the last La Nina period, no conclusions can be made about the long term results following the effects of the last La Nina period.

In the study by Smith, R. K. and Benson, A. P (2001) they also state that there is a need for constant one month data for extra exposed sites. They also state that frequent monitoring of beaches is usually both time consuming and costly. From the results in this part of the study a conclusion can be made that CoastSnap data could be a good alternative and making it easier to preform constant monitoring for exposed locations.

### **7.1.3 Error analysis**

The main data in this part of the report is the beach width. This is gathered by rectifying images and mapping the shorelines. This process is described in the methodology part. There could be errors in the measuring of the GPS points related to the exact positions in the image. If this would be a bit off there would be errors with how well the real world coordinates are related to the pixels in the photograph. That the distances on the image is measured correctly is important for the data to be correct since this is a distance measured in from the photograph. When the shoreline is mapped there is also a potential small error in that they were mostly done by hand. It is up to the one mapping the shoreline if it seems to be mapped correctly.

### **7.1.4 For future studies**

In future studies with CoastSnap data it would be interesting to include meteorological data as well as near shore wave data. This to see how well specific erosion episodes can be investigated.

It would also be interesting to use CoastSnap data for longer periods. Fore once with the intention to investigate a previous or following El Nino period as well, to investigate the more long term impacts of the last La Nina event. One example could be in the future when a El Nino period has developed and come to an end, add this data to the investigated period in this report. Since all the sites are up and running, data should be collected for all these beaches. It would be very interesting to see the potential recovery of these study sites in the near future.

Even though the data collected in this report seems to be sufficient, there is always going to be a liability with community collected data. It would be interesting to investigate more how to engage more people, and investigate how to minimize the liability of this parameter in the future.

From the results it is hard to give any clear recommendations for how the study sites should be managed in the future. Especially since as noted no real conclusions can be made about

the long term effects of the last La Nina period. But what could be noted for Stockton and Blacksmiths Beach is that the breakwalls seems to be working at preventing erosion. And Manly beach also seems to experience less erosion due to it 's more protected environment compared to it 's neighboring beach North Narrabeen Beach. Therefore one good solution in these wave-dominated areas to prevent erosion seems to be breakwalls.

### **7.1.5 Conclusions**

From the results it can be seen that the study sites are showing what is expected from previous research of what 'should' happen during a La Nina phase. From the data a connection between wave height and shoreline recession can also be seen, strengthening the claim that CoastSnap data can be used for research on coastal erosion. The quality and quantity of the data used is concluded to be good enough for this kind of research and concluded to show reliable results. From the results in this study it can be said that citizen data from CoastSnap does show reliable results regarding beach erosion on Australia's East coast during the last La Niña period.

## **7.2 Part 2: Shoreline modeling**

### **7.2.1 Initial model**

The first ever model run on an equilibrium shoreline model including all available citizen supplied shoreline data from CoastSnap, together with inshore location wave data, offered promising insights on shoreline change prediction. Seen in Table 8, the hindcast findings suggests impressive performance metrics.

The model aligned within the uncertainty range of shoreline measurements ( $\pm dx$ ) for about 77% of the time, which demonstrates high reliability in predicting shoreline positions. Furthermore, the model showed an overall correlation coefficient of 0.68, indicating a moderate yet evident connection between predicted and observed values. NMSE hovers around 0.5 m, indicating the model's estimated deviations from the observed data is reasonable.

When evaluated against a baseline model, represented by a linear trend, the model showed significant improvement as portrayed by the BSS being close to 0.62. This improvement shows the model's ability to capture complex shoreline dynamics beyond simplistic linear projections.

### **7.2.2 Test cases**

#### **1) How much data from CoastSnap is needed to train ShoreFor v1.0?**

Model runs with various sampling frequencies of shoreline data shows that the model performance do not significantly respond to the different chosen time intervals as each metric only differ modestly, which can be seen in table 9. However, there is indication of improvement in model performance and stronger correlations with the actual observed values with higher sampling frequency hence to slightly increasing BSS and r-values. This could be explained based on common principle within data science and statistics, as decreasing intervals in data collection tends to capture more minor and rapid changes or variations in the data pattern. Therefore, while wider intervals shows improved model performance metrics, narrower intervals may capture more detailed dynamics.

This might be an indication of the importance of finding a balance between data resolution and predictive accuracy when calibrating shoreline prediction models.

These findings show that the model shows very little sensitivity to data sampling frequencies. However, compared to the initial model that produced satisfying hindcast results with the complete data set, shoreline data sampling with time intervals  $\geq 7$  seems to be needed to achieve good model results. This is notably observed in the BSS, which for the initial model stands at a value greater than 0.6, whereas for all test runs with different sampling frequencies, it remains under 0.6. This could be considered a drawback for the purpose of modeling future shoreline change with public data collection. Manly beach has proven to be one of the places where the community have shown most interest in contributing to CoastSnap. However, at locations where interest is lower where uncertainties and gaps in data sampling becomes higher, citizen science data might not be sufficient for driving shoreline models to predict future shoreline change.

The hindcast results from model runs with various yearly duration lengths is presented in table 10 and showcases noticeable model performance differences. As the duration length increases, NMSE tends to decline which suggests improvement in accuracy. At the same time, the correlation coefficient decreases slightly, which means the correlation with the actual observed shoreline dynamics becomes weaker, with D\_1Y that even has an irregular deviation with a negative r-value. This suggests that calibration with duration of only one year is insufficient. All calibrations with durations 1:4 years generate BSS values  $> 0.3$ , indicating fair model performance, where the D\_1Y and D\_4Y models stand out with values above or close to 0.6 suggesting model performance is good.

Considering the negative R-squared value, one year of CoastSnap data used in this study is not adequate as the model fails to correlate the predicted values with the actual observed values. According to the BSS the D\_4 calibration that comes close to a value of 0.6 (except for 1 year but the liability of that calibration has already been ruled out), and overall the overall improvement in the remaining metrics with increasing duration length, it seems that a shoreline sampling duration of at least 4 years from this dataset is necessary to achieve satisfying hindcasts. In summary, the model seems to be relatively sensitive to data sampling durations and longer duration lengths show tendencies toward overall better model performance.

## **2) Is inshore/local wave conditions needed in order to get good model results when training the ShoreFor model with CoastSnap data?**

The hindcast results from calibrations with nearshore wave data and offshore wave data are presented for comparison in Table 11. The trends in the metrics show that training the model with inshore wave data generates slightly lower NMSE. This suggests a better predictive capability of the Initial model in estimating deviations from the observed shoreline data. It also shows that the model run with nearshore wave location provided higher correlation coefficient values and PTC, which also indicates stronger predictive tendencies when compared to the model run with offshore wave location. While the Offshore model has a marginally higher BSS, both models exhibit values  $> 0.6$ , which means they both show a satisfactory level of predictive accuracy.

The overall findings suggest that while the results only differs slightly between the two calibrations, driving the model with the transformed nearshore wave data seems to improve the model

performance. Especially in terms of reducing prediction errors and strengthening the correlation between predicted and observed shoreline data. Although, the slightly higher BSS value suggest certain advantages for the model run with offshore wave data.

### 7.2.3 For future studies

In future studies, conducting additional calibrations with even longer durations and a mix of shorter and longer data sampling intervals could offer valuable insights. This exploration would help discern the impact of varied data lengths and intervals on the model's predictive capabilities. As citizen science data can be a liable source of data gathering, exploring diverse calibration scenarios to see if the model is less sensitive to data sampling frequency when longer sets of data are available (and vice versa) would be interesting for further research. Inspiration can be found in the 2013 paper by Kristen et. al (2013) where similar calibrations were made in order to test model performance.

Another valuable aspect to explore would be to test the model using data from different study sites. Even though the data used in this study has proven sufficient for the For the ShoreFor model to generate dependable hindcasts, relying on community-based data always presents challenges in consistently collecting adequate information. It would be interesting to observe how the model reacts with data from a beach that generates less frequent data or, for some reason, has significant gaps in the data. Alternatively, testing the model with datasets that have intentionally missing data, such as calibrating a six-year dataset with occasional months of missing information. This approach might examine whether the data remains sufficient for modeling during unexpected events, like storms or similar occurrences, and the data collecting site would be temporarily inaccessible to the public.

### 7.2.4 Conclusions

Given results suggest that the community based data collection (CoastSnap) is a useful source of data to be able to train shoreline models with. After examining data degradation by testing different timeframes, it is clear that having more data over a longer period of time is better for predicting shoreline changes accurately.

Using information from at least four years gives good results. The longer we use this data to fine-tune the model, the better it will probably get at predicting how the shoreline will change in the future. Data sampling frequency proved to be of less importance but intervals  $> 7$  days seems to improve model performance.

Regarding forcing observations and whether offshore wave locations is sufficient or if the wave information has to be transformed into nearshore locations, it appears that the difference is not significantly substantial. However, using nearshore waves seems to enhance the model accuracy somewhat.

So, for the ShoreFor model to make reliable predictions about shoreline positions with shoreline data from CoastSnap, at least four years worth of data with a data sampling frequency  $> 7$  days seems ideal, and both nearshore and offshore wave information can be considered.

## 8 Bibliography

Aagaard, T., Greenwood, B. and Nielsen, J. (1997) 'Mean currents and sediment transport in a rip channel', *Marine Geology*, 140, pp. 25-45. <https://www.sciencedirect.com/science/article/pii/S002532279700025X>.

Allan, T. W., Rangel-Buitrago, N., Pranzini, E. and Anfuso, G. (2017) 'The management of coastal erosion', *Ocean & Coastal Management*, 156, pp. 4-20. Available at: <https://www.sciencedirect.com/science/article/pii/S0964569116304227>.

Spivak, A. C., Sanderman, J., Bowen, J. L., Canuel, E. A. and Hopkinson, C. S. (2019) 'Global-change controls on soil-carbon accumulation and loss in coastal vegetated ecosystems', *Nature Geoscience*, 12, pp. 685-692. Available at: <https://par.nsf.gov/servlets/purl/10132019>.

Deburghraeve, A., Robinet, A., Lecacheux, S., Bouvier, C., Simon, E. and Rosebery, D. (2023) 'Monitoring shoreline rotation with a CoastSnap system at the mesotidal embayed beach of Lafite-nia, France', in *Coastal Sediments 2023, Apr 2023, New Orleans (Louisiana), United States*. Available at: <https://hal.science/hal-04008708/document>.

Apple maps (2023).

Barnes, M. P., Andrews, M. and Fisk, G. (2011) 'Managing the Sunshine Coast shoreline erosion threat', in *Coasts and Ports 2011: Diverse and Developing: Proceedings of the 20th Australasian Coastal and Ocean Engineering Conference and the 13th Australasian Port and Harbour Conference*, Engineers Australia. Available at: <https://search.informit.org/doi/pdf/10.3316/informit.67503057816595>.

Bracs, M. A., Turner, I. L., Splinter, K. D., Short, A. D. and Mortlock, T. R. (2016) 'Synchronised patterns of erosion and deposition observed at two beaches', *Marine Geology*, 380, pp. 196-204. Available at: <https://www.sciencedirect.com/science/article/pii/S0025322716300706>.

Bryant, E. (1983) 'Regional sea level, Southern Oscillation and beach change, New South Wales, Australia', *Nature*, 30, pp. 213-216.

Bureau of Meteorology (2023) 'Record-breaking La Niña events', *Bureau of Meteorology*. Available at: <http://www.bom.gov.au/climate/enso/history/La-Nina-2010-12.pdf>.

Carley, J.T., Coghlan, I.R., Flocard, F., Cox, R.J. and Shand, T.D. (2003) *Establishing the Design Scour Level for Seawalls*, Water Research Laboratory, School of Civil and Environmental Engineering, UNSW Australia.

Elrick-Barr, C. E., Clifton, J., Cuttler, M., Perry, C. and Rogers, A. A. (2023) 'Understanding coastal social values through citizen science: The example of CoastSnap in Western Australia', *Ocean & Coastal Management*, 238. <https://www.sciencedirect.com/science/article/pii/S0964569123000881>.

Ummenhofer, C. C., Sen Gupta, A., England, M. H., Taschetto, A. S., Briggs, P. R. and Raupach,

- M. R. (2015) ‘How did ocean warming affect Australian rainfall extremes during the 2010/2011 La Niña event?’, *Geophysical Research Letters*, 42, pp. 9942-9951. Available at: <https://agupubs.onlinelibrary.wiley.com/doi/full/10.1002/2015GL065948>.
- Drummond, C. D., Carley, J. T., Vos, K. and Lanceman, D. (2020) *Blacksmiths Beach surf amenity assessment*, UNSW Water Research Laboratory. Available at: <https://www.wrl.unsw.edu.au/sites/wrl/files/uploads/Publications/WRL-TR2020-14-Blacksmiths-Beach-surf-amenity-assessment.pdf>.
- Wang, C. and Picaut, J. (2004) *Understanding ENSO Physics—A Review*, in *Earth’s Climate: The Ocean-Atmosphere Interaction, Geophysical Monograph Series*, 147, pp. 21-48. [https://www.researchgate.net/profile/Chunzai-Wang/publication/277686335\\_Understanding\\_ENSO\\_physics\\_-\\_A\\_review/links/55b8e76308aec0e5f43ba7c0/Understanding\\_-\\_ENSO\\_-\\_physics\\_-\\_A\\_-\\_review.pdf](https://www.researchgate.net/profile/Chunzai-Wang/publication/277686335_Understanding_ENSO_physics_-_A_review/links/55b8e76308aec0e5f43ba7c0/Understanding_-_ENSO_-_physics_-_A_-_review.pdf).
- City of Newcastle (2020) ‘Stockton Bight Sand Movement Study’, Report #: P19028\_R4.00, *City of Newcastle*. Available at: <https://newcastle.nsw.gov.au/Newcastle/media/Documents/environment/Our%20Coastline%20-%20Documents/Stockton%20Erosion%20Response%20-%20Documents/FINAL-StocktonBightStudy-R4-00.pdf>.
- Coast Snap (2023a) ‘Background’. Available at: <https://www.CoastSnap.com/explore/background>.
- Coast Snap database (2023). Available at: <https://www.spotteron.com/CoastSnap/menu>.
- Davidson, M., Splinter, K. and Turner, I. (2013) ‘A simple equilibrium model for predicting shoreline change’, *Coastal Engineering*, 73, pp. 191–202.
- Davidson, M. and Turner, I. (2009) ‘A behavioral template beach profile model for predicting seasonal to interannual shoreline evolution’, *Journal of Geophysical Research: Earth Surface*, 114(F1).
- Dean, R. G. (1977) *Equilibrium beach profiles: US Atlantic and Gulf coasts*, Department of Civil Engineering and College of Marine Studies, University of Delaware.
- Defeo, O., McLachlan, A., Schoeman, D. S., Schlacher, T., Dugan, J., Jones, A., Lastra, M., Scapini, F. (2008) ‘Threats to sandy beach ecosystems: A review’, *Estuarine, Coastal and Shelf Science*, Vol, pp. 2-12. [https://www.researchgate.net/profile/Mariano-Lastra/publication/228727544\\_Threats\\_to\\_sandy\\_beach\\_ecosystems\\_A\\_review/links/5c1b52d5458515a4c7eb217a/Threats\\_-\\_to\\_-\\_sandy\\_-\\_beach\\_-\\_ecosystems\\_-\\_A\\_-\\_review.pdf](https://www.researchgate.net/profile/Mariano-Lastra/publication/228727544_Threats_to_sandy_beach_ecosystems_A_review/links/5c1b52d5458515a4c7eb217a/Threats_-_to_-_sandy_-_beach_-_ecosystems_-_A_-_review.pdf).
- Drummond, C. D., Carley, J. T., Vos, K., Lanceman, D. (2020) *Blacksmiths Beach surf amenity assessment*, UNSW Water Research Laboratory. Available at: <https://www.wrl.unsw.edu.au/sites/wrl/files/uploads/Publications/WRL-TR2020-14-Blacksmiths-Beach-surf-amenity-assessment.pdf>.
- King, E. V., Conley, D. C., Masselink, G. and Leonardi, N. (2021) ‘Predicting Dominance of Sand Transport by Waves, Tides, and Their Interactions on Sandy Continental Shelves’, *Journal of Geophysical Research: Oceans*, 126. Available at: <https://agupubs.onlinelibrary.wiley.com/doi/pdf/10.1029/2021JC017200>.

- Miot da Silva, G., Siadat Mousavi, S. M., Jos, F. (2012) ‘Wave-driven sediment transport and beach-dune dynamics in a headland bay beach’, *Marine Geology*, 323-325, pp. 29-46. Available at: <https://www.sciencedirect.com/science/article/pii/S0025322712001661>.
- Hanson, H. and Lindh, G. (1993) ‘Coastal Erosion: An Escalating Environmental Threat’, *Ambio*, 22, pp. 188-195. Available at: <https://www.jstor.org/stable/4314068>.
- Hanson, H. (1989) ‘GENESIS: a generalized shoreline change model’, *Journal of Coastal Research*, 5 (1), pp. 1–27.
- Harley, M. D., Turner, I. L., Short, A. D. and Ranasinghe, R. (2010) ‘Interannual variability and controls of the Sydney wave climate’, *Int. J. Climatol*, 30, pp. 1322–1335. *Holocene evolution of the wave-dominated embayed Moruya coastline, southeastern Australia: Sediment sources, transport rates and alongshore interconnectivity*, Quaternary Science Reviews.
- Harley, M. D. and Kinsela, M. A. (2022) ‘CoastSnap: A global citizen science program to monitor changing coastlines’, *Continental Shelf Research*, 245.
- Harley, M. D., Kinsela, M. A., Sánchez-García, E. and Vos, K. (2019) ‘Shoreline change mapping using crowd-sourced smartphone images’, *Coastal Engineering*, 150, pp. 175-189. Available at: <https://www.sciencedirect.com/science/article/pii/S0378383918304551>.
- James, R. J. (2000) ‘From beaches to beach environments: linking the ecology, human-use and management of beaches in Australia’, *Ocean & Coastal Management*, 43, pp. 495-514. Available at: <https://www.sciencedirect.com/science/article/pii/S0964569100000405>.
- King, E. V., Conley, D. C., Masselink, G. and Leonardi, N. (2021) ‘Predicting Dominance of Sand Transport by Waves, Tides, and Their Interactions on Sandy Continental Shelves’, *Journal of Geophysical Research: Oceans*, 126. Available at: <https://agupubs.onlinelibrary.wiley.com/doi/pdf/10.1029/2021JC017200>.
- Komar, P. D., Allan, J., Das-Me’ndez, G. M., Marra, J. J. and Ruggiero, P. (2000) ‘El Niño and La Niña: Erosion Processes and Impacts’. Available at: [https://www.researchgate.net/profile/Jonathan-Allan-4/publication/269125506\\_El\\_Niño\\_and\\_La\\_Niña\\_Erosion\\_Processes\\_and\\_Impacts/links/5e1f9fe929bf1e1fab4cfb4/El-Niño-and-La-Niña-Erosion-Processes-and-Impacts.pdf](https://www.researchgate.net/profile/Jonathan-Allan-4/publication/269125506_El_Niño_and_La_Niña_Erosion_Processes_and_Impacts/links/5e1f9fe929bf1e1fab4cfb4/El-Niño-and-La-Niña-Erosion-Processes-and-Impacts.pdf).
- Larson, P. M., Nam, P.T., Hanson, H. and Xua Hoan, L. (2011) ‘A numerical model of beach morphological evolution due to waves and currents in the vicinity of coastal structures’, *Coastal Engineering*, 58 (9), pp. 863–876.
- Leatherman, S. P., Zhang, K. and Douglas, B. C. (2000) ‘Sea level rise shown to drive coastal erosion’, *Eos, Transactions American Geophysical Union*, 81, pp. 55-57. Available at: <https://agupubs.onlinelibrary.wiley.com/doi/abs/10.1029/00EO00034>.
- Liu, Y., Huang, H., Qiu, Z. and Fan, J. (2013) ‘Detecting coastline change from satellite images based on beach slope estimation in a tidal flat’, *International Journal of Applied Earth Observation and Geoinformation*, 23, pp. 165-176. Available at: <https://www.sciencedirect.com/science/article/>

pii/S0303243412002450.

Mortlock, T. R. and Goodwin, I. D. (2014) ‘Nearshore parametric wave data for ARC and OEH project sites’, Marine Climate Risk, Climate Futures and Department of Environment and Geography, Macquarie University, North Ryde, 2109, Australia.

NOAA Climate (2023b) ‘Equatorial Pacific Sea Surface Temperatures (SST)’. <https://www.ncei.noaa.gov/access/monitoring/enso/sst>.

NOAA Climate (2023c) ‘ENSO and Climate Change: What does the new IPCC report say?’. Available at: <https://www.climate.gov/news-features/blogs/enso/enso-and-climate-change-what-does-new-ipcc-report-say>.

NOAA Climate (2015) ‘NOAA study finds marshes, reefs, beaches can enhance coastal resilience’. Available at: <https://coast.noaa.gov/states/fast-facts/natural-infrastructure.html>

Oliver, T. S., Tamura, T., Brooke, B. P., Short, A. D., Kinsela, M. A., Woodroffe, C. D. and Thom, B. G. (2020).

Phinn, S. R. and Hastings, P. A. (1992) ‘Southern Oscillation influences on the wave climate of south-eastern Australia’, *J. Coast. Res.*, 8, pp. 579–592.

Russell, P. E. (1993) ‘Mechanisms for beach erosion during storms’, *Continental Shelf Research*, 13, pp. 1243–1265. Available at: <https://www.sciencedirect.com/science/article/pii/027843439390051X>.

Smith, R. K. and Benson, A. P. (2001) ‘Beach profile monitoring: How frequent is sufficient?’, *J. Coast. Res.*, 34, pp. 573–579. Available at: <https://www.jstor.org/stable/25736322>.

Song, L., Chen, S., Chen, W. and Chen, X. (2016) ‘Distinct impacts of two types of La Niña events on Australian summer rainfall’, *International Journal of Climatology*, 37, pp. 2532–2544. Available at: <https://rmets.onlinelibrary.wiley.com/doi/abs/10.1002/joc.4863>.

Splinter, K. D., Turner, I. L., Davidson, M. A., Barnard, P., Castelle, B. and Oltman-Shay, J. (2014) ‘A generalized equilibrium model for predicting daily to interannual shoreline response’, *J. Geophys. Res. Earth Surf.*, 119, pp. 1936–1958, doi:10.1002/2014JF003106.

Troels Aagaard, Greenwood, B. and Nielsen, J. (1997) ‘Mean currents and sediment transport in a rip channel’, *Marine Geology*, 140, pp. 25–45. Available at: <https://www.sciencedirect.com/science/article/pii/S002532279700025X>.

Troels Aagaard, Greenwood, B. and Hughes, M. (2013) ‘Sediment transport on dissipative, intermediate and reflective beaches’, *Earth-Science Reviews*, 124, pp. 32–50. Available at: <https://www.sciencedirect.com/science/article/pii/S0012825213000925>.

Walsh, K. J. E., McBride, J. L., Klotzbach, P. J., Balachandran, S., Camargo, S. J., Holland, G., Knutson, T. R., Kossin, J. P., Lee, T.-c., Sobel, A. and Sugi, M. (2015) ‘Tropical cyclones and climate change’, *WIREs Climate Change*, 7, pp. 65–89. Available at: <https://wires.onlinelibrary>.

wiley.com/doi/abs/10.1002/wcc.371.

Wright, L.D., Short, A.D. and Green, M.O. (1985) 'Short-term changes in the morphodynamic states of beaches and surf zones; an empirical predictive model', *Marine Geology*, 62, pp. 339–364.

Wright, L. D., Chappell, J., Thom, B. G., Bradshaw, M. P. and Cowell, P. (1979) 'Morphodynamics of reflective and dissipative beach and inshore systems: Southeastern Australia', *Marine Geology*, 32, pp. 105-140. Available at: <https://www.sciencedirect.com/science/article/pii/002532277990149X>.

Yates, M. L., Guza, R. T., O'Reilly, W. C. (2009). *Equilibrium shoreline response: Observations and modeling* Observations and modeling', *J. Geophys. Res.*, 114, C09014, doi:10.1029/2009JC005359.